

Brain networks for temporal adaptation, anticipation, and sensory-motor integration in rhythmic human behavior

Bronson B. Harry^a, Daniel S. Margulies^{b,c}, Marcel Falkiewicz^c, Peter E. Keller^{a,d,*}

^a The MARCS Institute for Brain, Behaviour and Development, Western Sydney University, Sydney, Australia

^b Integrative Neuroscience and Cognition Center, Centre National de la Recherche Scientifique (CNRS) and Université de Paris, Paris, France

^c Max Planck Research Group for Neuroanatomy and Connectivity, Max Planck Institute for Human Cognitive and Brain Sciences, Leipzig, Germany

^d Center for Music in the Brain, Department of Clinical Medicine, Aarhus University & The Royal Academy of Music Aarhus/Aalborg, Aarhus, Denmark

ARTICLE INFO

Keywords:

Sensorimotor synchronization

Temporal prediction

Error correction

Sensory-motor integration

fMRI

Functional connectivity

ABSTRACT

Human interaction often requires the precise yet flexible interpersonal coordination of rhythmic behavior, as in group music making. The present fMRI study investigates the functional brain networks that may facilitate such behavior by enabling temporal adaptation (error correction), prediction, and the monitoring and integration of information about 'self' and the external environment. Participants were required to synchronize finger taps with computer-controlled auditory sequences that were presented either at a globally steady tempo with local adaptations to the participants' tap timing (Virtual Partner task) or with gradual tempo accelerations and decelerations but without adaptation (Tempo Change task). Connectome-based predictive modelling was used to examine patterns of brain functional connectivity related to individual differences in behavioral performance and parameter estimates from the adaptation and anticipation model (ADAM) of sensorimotor synchronization for these two tasks under conditions of varying cognitive load. Results revealed distinct but overlapping brain networks associated with ADAM-derived estimates of temporal adaptation, anticipation, and the integration of self-controlled and externally controlled processes across task conditions. The partial overlap between ADAM networks suggests common hub regions that modulate functional connectivity within and between the brain's resting-state networks and additional sensory-motor regions and subcortical structures in a manner reflecting coordination skill. Such network reconfiguration might facilitate sensorimotor synchronization by enabling shifts in focus on internal and external information, and, in social contexts requiring interpersonal coordination, variations in the degree of simultaneous integration and segregation of these information sources in internal models that support self, other, and joint action planning and prediction.

1. Introduction

Diverse human activities rely on precise, yet flexible coordination of behavior across two or more individuals in real time. Such interpersonal temporal alignment—evident in rhythmic activities ranging from marching and rowing to collective music-making and dance—serves cultural functions in promoting social bonding and cooperative behavior (D'Ausilio et al., 2015; Shamay-Tsoory et al., 2019). The capacity for rhythmic interpersonal coordination is based on psychological mechanisms that enable individuals to anticipate and adapt to each other's action timing, and to monitor their own performance whilst simultaneously monitoring and integrating information about their co-actors'

behavior (Gallotti et al., 2016; Keller et al., 2014; Konvalinka et al., 2010). Previous neuroimaging research has identified associations between these mechanisms and multiple brain regions engaged in basic sensory and motor processing, as well as higher-level cognitive and social-emotional processes (e.g., Chauvigne et al., 2014; Fairhurst et al., 2013, 2014; Konvalinka et al., 2014; Pecenkova et al., 2013; Repp and Su, 2013). The present study investigates how these brain regions form networks that interact to support temporal adaptation, anticipation, and the processing of information about one's own actions and relevant external events during real-time coordination.

* Corresponding author. Center for Music in the Brain, Department of Clinical Medicine, Health, Aarhus University, Universitetsbyen 3, Building 1710, Aarhus, C 8000, Denmark.

E-mail addresses: bronson.harry@gmail.com (B.B. Harry), p.keller@clin.au.dk (P.E. Keller).

<https://doi.org/10.1016/j.neuropsychologia.2023.108524>

Received 5 August 2022; Received in revised form 21 January 2023; Accepted 22 February 2023

Available online 1 March 2023

0028-3932/© 2023 The Authors. Published by Elsevier Ltd. This is an open access article under the CC BY-NC-ND license (<http://creativecommons.org/licenses/by-nc-nd/4.0/>).

1.1. Temporal adaptation & anticipation

Fundamental mechanisms of temporal adaptation detect discrepancies in timing (i.e., asynchronies) between an individual's actions and external events, and implement reactive error correction to compensate for these asynchronies via adjustments to the timing of the individual's upcoming actions (Mates, 1994b; Praamstra et al., 2003; Repp and Keller, 2008). Behavioral studies of this process suggest that adjustments to the phase alignment (i.e., amount of lead or lag) of internal time-keeping mechanisms that underlie rhythmic actions operate automatically, while adjustments to timekeeper period (which determines tempo) require attention and effort (Repp, 2005; Repp and Keller, 2004).

Anticipatory mechanisms that support rhythmic coordination exploit temporal relations between sequential events (e.g., patterns of tempo change found in expressively performed music) to generate predictions about the timing of future events (Keller, 2008; Konvalinka et al., 2010; Pecenka and Keller, 2011). Such temporal prediction is characterized by individual differences related to working memory and the strength of covert motor simulation processes that drive mental imagery for upcoming actions (Colley et al., 2018; Keller, 2012a; Pecenka and Keller, 2011).

A growing body of research suggests that temporal adaptation and anticipation work together to facilitate rhythmic coordination by allowing one's own actions to be planned relative to predictions about the timing of external event sequences, and to be adjusted in response to asynchronies that arise due to inaccurate predictions and inherent variability in movement control (Mills, van der Steen et al., 2015; van der Steen and Keller, 2013). Furthermore, the balance between adaptation and anticipation is regulated via attentional processes that respond to momentary task demands associated with simultaneously monitoring and integrating information about one's own actions and external events (Mills et al., 2019; van der Steen et al., 2015a). Individual differences in these processes determine rhythmic coordination skills and can thereby influence social interaction in everyday contexts (D'Ausilio et al., 2015; Keller et al., 2014).

Functional magnetic resonance imaging (fMRI) research has examined brain activity associated with temporal adaptation and anticipation in conjunction with behavioral sensorimotor synchronization tasks that require participants to produce simple movements (e.g., finger taps) in time with auditory pacing sequences. Studies of adaptation have employed computer-controlled 'virtual partners' that are programmed to react to the human participants' tap timing by implementing varying degrees of error correction, while studies of anticipation have used pacing sequences containing systematic patterns of gradual tempo change (Dumas et al., 2014; Dumas et al., 2019; Fairhurst et al., 2013, 2014; Miyata et al., 2022; Pecenka et al., 2013). This work suggests that adaptation and anticipation are associated with activity in partially overlapping networks of widely distributed brain areas that feature prominently in the large body of neuroimaging research on sensorimotor synchronization and rhythm perception and production more generally.

1.2. Brain networks for rhythmic behavior

Key players in the literature on rhythmic behavior include motor-related cortical regions (e.g., premotor cortex and supplementary motor area) and subcortical structures (basal ganglia and cerebellum) that become functionally coupled with sensory areas and other cortical regions, including auditory cortex and primary motor cortex, depending on specific task demands (for reviews, see Cannon and Patel, 2021; Chauvigne et al., 2014; Comstock et al., 2018; Coull et al., 2011; Levitin et al., 2018; Patel and Iversen, 2014; Repp and Su, 2013; Todd and Lee, 2015a; Vuust et al., 2022; Witt et al., 2008). Levels of activation and functional connectivity within and between these regions are modulated by structural features of the task, concurrent demands, and the musical

experience of participants (e.g., Chen et al., 2008; Grahn and Brett, 2007; Matthews et al., 2020; Pecenka et al., 2013; Penhune et al., 1998; Pollok et al., 2005; Todd and Lee, 2015b; Toiviainen et al., 2020; Vuust et al., 2006). Such dependencies suggest that studying the brain networks for sensorimotor synchronization is best done using tasks that capture a range of timing demands, and by focusing on individual differences under conditions of varying cognitive load.

Numerous related studies have addressed distinctions between the processing of rhythms with a regular periodic beat structure versus irregularly timed rhythms, or rhythmic movements that are internally (self) paced versus externally paced by auditory sequences. Although less work has addressed temporal adaptation and anticipation directly, the findings of studies on rhythmic regularity and external versus internal pacing are potentially informative for identifying networks for temporal adaptation and anticipation (which are not relevant in the case of internally paced action) and assessing effects of cognitive load (which is higher for irregular than regular patterns).

Related research suggests that the reactive error correction processes underpinning adaptive timing are supported by extensive subcortical and cortical networks (Bijsterbosch et al., 2011; Fairhurst et al., 2013, 2014; Jäncke et al., 2000; Oullier et al., 2005; Praamstra et al., 2003; Rao et al., 1997; Stephan et al., 2002). There is considerable overlap in regions implicated in phase correction and period correction, including the cerebellum, premotor cortex, inferior frontal gyrus, dorsolateral and ventrolateral prefrontal cortices, temporoparietal junction, anterior cingulate, and anterior insula (Table S1 in Supplementary Materials). However, there is evidence for partial neurophysiological distinction between the two types of error correction to the extent that phase correction additionally recruits the basal ganglia (particularly the caudate), inferior parietal lobule, pre-supplementary motor area, superior temporal gyrus, primary motor cortex, posterior cingulate cortex, and precuneus (Fairhurst et al., 2013, 2014; Stephan et al., 2002), while period cortex involves the supplementary motor area and posterior parietal cortex (Praamstra et al., 2003; Repp and Su, 2013). Furthermore, temporal prediction recruits a number of areas in common with those involved in temporal adaptation, but also calls on the putamen in the basal ganglia, the inferior and middle temporal gyri, superior parietal lobule, supramarginal gyrus, frontal pole, precentral gyrus, and middle and superior frontal gyri (Coull et al., 2011; Grahn and Rowe, 2013; Miyata et al., 2022; Pecenka et al., 2013; Schubotz, 2007). There is thus likely to be both noteworthy overlap and distinction in networks for temporal adaptation and anticipation.

Areas of overlap are well-situated to serve as hub regions that mediate the relationship between temporal adaptation and anticipation. Some of these regions play a role in sensory-motor integration, notably the temporoparietal junction, middle cingulate gyrus, inferior parietal lobule, posterior parietal cortex, precuneus, premotor cortex, and the supplementary motor area (see Todd and Lee, 2015a; Witt et al., 2008) (Table S1). These possible hub regions are also sensitive to modulations in rhythmic regularity (related to beat salience and the complexity of inter-stimulus interval duration ratios) and cognitive load (Alluri et al., 2012; Thaut et al., 2008; Toiviainen et al., 2020) (Table S1). Such dependencies highlight the potential relevance of the interplay between elementary sensory-motor processes and higher-level cognitive operations, including attention and working memory (Coull, 2004; Hill and Miller, 2010; Janata et al., 2002; Satoh et al., 2001), during sensorimotor synchronization. We assume that this interplay takes place via the reconfiguration of the brain's canonical resting-state networks, which comprise cortical and cerebellar sensory and motor-related regions, cingulo-opercular regions involved in conflict monitoring and error detection, fronto-parietal cognitive control regions, dorsal and ventral attention regions, and midline and lateral default mode regions linked to self-referential and social-cognitive processing (Cohen & D'Esposito, 2016; Deco et al., 2015; Dixon et al., 2017; Seitzman et al., 2019; Sporns, 2013; Wang et al., 2021).

Temporal adaptation and anticipation during sensorimotor

synchronization might therefore be supported by a core network of hub regions that modulates functional connectivity within and between the brain's resting-state networks and additional sensory-motor regions and sub-cortical structures depending on concurrent cognitive demands and the individual differences in coordination skill.

Studies of sensorimotor synchronization with virtual partners have yielded results that are consistent with such reconfiguration. One study found that small shifts in the degree of adaptive timing employed by the virtual partner led to large-scale switches from activation of regions predominantly within the default mode and somatomotor networks (including posterior cingulate cortex, precuneus, supplementary motor area, and primary motor and somatosensory cortices) to increased activation of regions in frontoparietal control and salience networks (e. g., dorsomedial prefrontal cortex and anterior insula) (Fairhurst et al., 2013). In a related study, brain activation patterns differed depending on the coordination strategies that individuals used when interacting with uncooperative virtual partners (Fairhurst et al., 2014). Specifically, the prioritization of stabilizing one's own performance, presumably via internal focus, was associated with activation in the pre-supplementary motor area and precuneus. Such findings have been taken to indicate that network configuration plays a role in regulating the monitoring and integration of information about 'self' and 'other' (i.e., another human or virtual partner) depending on one's own adaptation and anticipation capacities, as well as the cooperativity of one's partner (Keller et al., 2014; Keller et al., 2016; Lieberman-Jordanidis et al., 2021).

Simultaneous self-other integration and segregation can be viewed as a specific form of balancing internal (self) versus external (other) sources of information (Novembre et al., 2016). Expertise in domains where rhythm is a key element may be characterized by the strategic modulation of this balance. For instance, a study with shamanic practitioners found that trance states induced by rhythmic drum sounds were associated with increased functional connectivity between a posterior cingulate seed region in the default mode network and control-related network regions. This pattern of between-network coupling was, furthermore, accompanied by perceptual decoupling from the acoustic input, indicated by decreased connectivity in the auditory pathway (presumably facilitating an internally oriented mode of processing that promotes insight) (Hove et al., 2016). Moreover, with respect to individual differences, an EEG study of dyadic finger tapping found distinct types of brain network coupling depending on whether individuals engaged in high or low levels of mutual adaptation (Heggli et al., 2020). High adaptation was associated with relatively strong coherence in a right-lateralized network spanning auditory cortex, somatosensory cortex, temporoparietal junction, middle temporal gyrus, inferior parietal cortex, supramarginal gyrus, and precuneus. The direction of information flow within this network also varied as a function of adaptation strategy. The foregoing suggests that sensorimotor synchronization skill may be reflected in flexibility in the functional coupling of brain networks to optimize focus on external versus internal sources of information depending on the task at hand.

1.3. Present aim

Previous fMRI research examined adaptation and anticipation in separate studies and identified brain networks only qualitatively based on regional activation. The current study addresses the open question of how adaptation and anticipation interact, and how the related brain regions form functional networks that communicate within and between one another in order to produce precise yet flexible synchronization behavior. To this end, we combine advances in brain network identification (Finn et al., 2015; Rosenberg et al., 2017; Rosenberg et al., 2016) with computational modelling of behavior using the adaptation and anticipation model (ADAM) of sensorimotor synchronization (Harry and Keller, 2019; van der Steen et al., 2015a; van der Steen and Keller, 2013).

ADAM comprises an adaptation module that provides input to an

internal model of the 'self', which plays a role in action planning (Wolpert and Kawato, 1998), an anticipation module that informs an internal model of the 'other', for prediction of external sequential events (Wolpert et al., 2003), and a joint module that integrates the output of the 'self' and 'other' internal models via attentional regulation (Keller et al., 2016; cf. Müller et al., 2021; Pesquita et al., 2018) (see Fig. 1A). This joint internal model computes the discrepancy between outputs of the 'self' and 'other' internal models, and implements anticipatory error correction to reduce this discrepancy by adjusting one's own action plan in the 'self' internal model prior to action execution. In this conceptualization, the output the joint module represents the relative integration and segregation of information about self and other (Keller et al., 2016). ADAM differs from approaches that model phase and period relations (e. g., Heggli et al., 2019; Loehr et al., 2011; Mates, 1994a, 1994b; Schulze et al., 2005; Tognoli and Kelso, 2014) primarily through the inclusion of the anticipation module, which uses an extrapolation function for tempo-change prediction, and the joint module that combines these predictions with the output of the adaptation module (see section 2.4).

Applying ADAM to behavioral data allows the estimation of parameters that reflect individual participants' use of reactive (phase and period) error correction, temporal (stimulus) prediction, and anticipatory error correction, thus providing a window into self-other monitoring and integration capacities for real-time interpersonal coordination (Mills et al., 2019; van der Steen et al., 2015a; van der Steen et al., 2015b). To identify the brain networks associated with ADAM's adaptation, anticipation, and joint modules, we adopt a connectome-based predictive modelling approach (Finn et al., 2015; Rosenberg et al., 2016, 2017) that examines patterns of functional connectivity related to individual differences in behavioral measures and ADAM parameter estimates. These connectivity patterns were investigated across conditions of varying cognitive load to test their reliability and the degree to which they are modulated by attention.

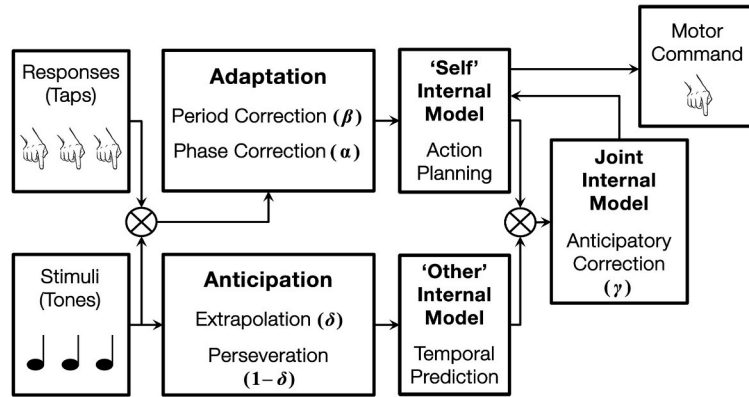
2. Methods

2.1. Study overview & design

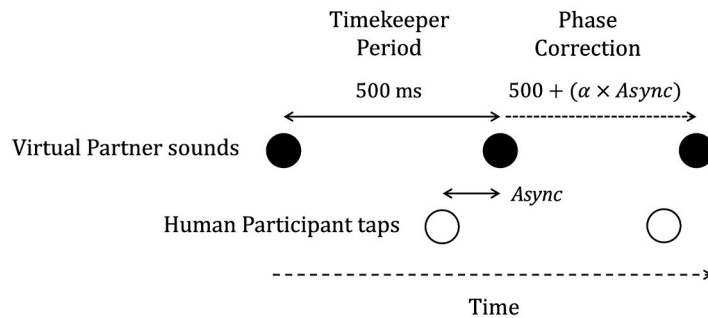
fMRI data were collected while participants completed two audio-motor sensorimotor synchronization tasks (Virtual Partner task and Tempo Change task) designed to assess temporal adaptation and anticipation under two cognitive load conditions (single task and dual task). The Virtual Partner task was used to examine parameters from the adaptation module of ADAM under steady tempo conditions that were not expected to show large effects of cognitive load (Repp and Keller, 2004). The Tempo Change task interrogated the ADAM's adaptation, anticipation, and joint modules under more demanding conditions that were expected to be susceptible to effects of cognitive load (Pecenka et al., 2013). This selection of tasks and modelling approach was based on previous behavioral work investigating individual differences in sensorimotor synchronization (see Harry and Keller, 2019).

The Virtual Partner task (Fig. 1B) was originally developed to evoke naturalistic corrective behavior where the participant and computer-controlled virtual partner mutually adapt to each other's timing (Repp and Keller, 2008). The task requires participants to synchronize finger taps with adaptive auditory pacing sequences generated by the virtual partner. In the current study, the virtual partner produced target sounds with a base inter-stimulus interval that was adjusted at each cycle by a fixed proportion of the asynchrony produced by the participant relative to the virtual partner's previous sound (Fairhurst et al., 2013; Mills et al., 2015; Repp and Keller, 2008). This proportion—effectively instantiating phase correction in the virtual partner—was set to different adaptivity values to create under-correcting, optimal-correcting, and over-correcting partners across conditions (Fairhurst et al., 2013). Estimates of human adaptation derived from participants should therefore generalize across a range of partners who vary in cooperativity. ADAM parameter estimates of phase correction and period correction were

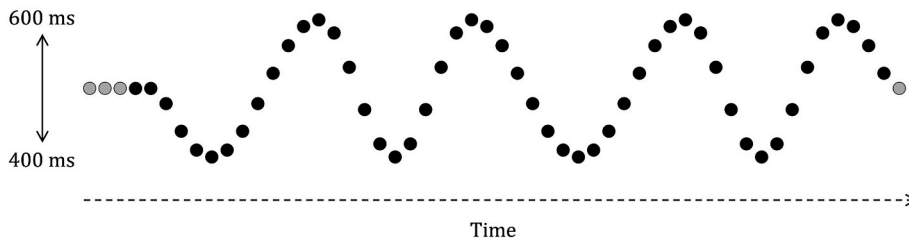
A. Adaptation & Anticipation Model (ADAM)



B. Virtual Partner Task



C. Tempo Change Task



computed for individual participants by fitting ADAM to behavioral data from each trial of the Virtual Partner task. The phase correction parameter (designated ' α ' in the model nomenclature) represents the proportion of each asynchrony that is reactively compensated for by the participant on average (via a local adjustment that leaves the base period of the internal timekeeper unchanged), reflecting the strength of sensory-motor coupling (Repp et al., 2012). The period correction parameter (β) represents the proportion of each asynchrony that is compensated for by globally increasing or decreasing the timekeeper period (Harry and Keller, 2019). Period correction is unnecessary and was not expected to come into play in the Virtual Partner task due to the regular tempo.

In the Tempo Change task (Fig. 1C), participants synchronized finger taps with auditory pacing sequences comprising inter-stimulus intervals that varied gradually (without adapting to participants' tap timing, in contrast to the Virtual Partner task) (Mills et al., 2015; Pecenka et al., 2013). The Tempo Change task was used to estimate participants' use of period correction (as above), as well as stimulus prediction and

Fig. 1. Schematic diagrams of the Adaptation and Anticipation Model (ADAM) of sensorimotor synchronization and the behavioral tasks. **A)** Adaptation and Anticipation Model (ADAM) architecture. Phase correction (α) and period correction (β) mechanisms in the 'adaptation' module influence action planning in a 'self' internal model. The 'anticipation' module controls the weighting (δ) of two processes, one entailing linear extrapolation of previous inter-onset intervals in the external sequence and the other copying the previous interval, which inform temporal predictions in an 'other' internal model. An anticipatory error correction mechanism (γ) a 'joint' internal model reduces discrepancies between (self) plans and (other) predictions before motor commands are issued. **B)** Virtual Partner task in which participants synchronize finger taps with computer-controlled auditory sequences that adapt to the participants to varying degrees (controlled by the phase correction parameter 'alpha', α). **C)** Tempo Change task, in which participants tap in time with auditory pacing sequences containing gradual accelerations and deceleration spanning 400–600 ms inter-onset intervals.

anticipatory error correction. ADAM's stimulus prediction parameter (δ) represents the degree to which participants exploit recent changes in the pacing sequence inter-stimulus intervals to predict the timing of upcoming sounds. This parameter weights the relationship between a linear extrapolation process based on preceding intervals versus a tracking process that copies the most recent interval (van der Steen and Keller, 2013). The anticipatory error correction parameter (γ) represents the degree to which discrepancies between the output of the adaptation and anticipation modules are corrected before the next movement is executed. The parameter estimate reflects the proportion of the discrepancy that is compensated for by adjusting one's own action plan before a motor command is issued (van der Steen et al., 2015a).

Participants completed both sensorimotor synchronization tasks under single-task (tapping only) and dual-task (tapping plus a secondary visual '1-back' working memory task) conditions. Previous work has shown that behavioral processes related to adaptation and anticipation show selective effects of a secondary task. Specifically, period correction is impaired to a greater degree than phase correction (Repp and Keller,

2004), and temporal prediction is impaired more than tracking (Pecenka et al., 2013). Here we extended the investigation to anticipatory error correction, and tested for changes in functional connectivity within and between brain networks associated with parameters from all ADAM modules.

2.2. Participants

Seventy-five right-handed participants (41 females and 34 males, aged 18–40 years) were recruited via social media and on-campus flyers at Western Sydney University. Individuals with varying amounts of musical experience were included to increase the likelihood that the participant sample represented a range of sensorimotor synchronization abilities. Thirty-five musicians had 5–22 years of experience at playing a musical instrument and had either engaged in musical instruction at a tertiary level or were professionally active. The remaining 40 individuals had no formal music training beyond mandatory classroom music education in primary/secondary school. All participants had participated in previous sensorimotor synchronization experiments, and were drawn from a dedicated project database maintained at the MARCS Institute for Brain, Behaviour and Development. Participants received payment for taking part in the experiment. The study was approved by the Human Research Ethics Committee at Western Sydney University (protocol number H10487), and all participants provided informed written consent.

2.3. Procedure & materials

After screening, each participant completed a practice session, which included tasks identical to those administered in the scanner, one week prior to the imaging session. Both practice and scanning sessions comprised multiple runs of the two auditorily paced synchronized finger-tapping tasks (Virtual Partner task and Tempo Change task) presented under the two cognitive load conditions (single task and dual task) in a blocked design. Given that the current study was primarily focused on individual differences, all participants were presented these tasks with the same fixed order of trials. Participants first completed both finger-tapping tasks in the single-task condition, starting with the Virtual Partner task, and then completed the dual-task condition with the same order of trials presented in the single-task condition. Each of the four task and condition combinations was presented in a separate run.

Task runs consisted of 9 trials that each started with four cowbell lead-in stimuli presented with inter-stimulus intervals of 500 ms, followed by a sequence of 48 target woodblock stimuli for which the timing was determined by the particular task (see below). Participants were instructed to begin tapping with their right index finger on the third cowbell sound and to continue tapping until the trial was terminated by a pure tone ‘beep’ presented 500 ms after the last woodblock sound. After each trial, participants rated the difficulty of the trial on a scale of 1 (very easy) to 4 (very hard). Participants indicated this response with a four-button response box held in their left hand. Each trial was separated by a 15 s rest block.

The cowbell and woodblock stimuli were generated by a Roland TD-9 Percussion Sound Module that was situated in a control room adjacent to the scanning room. The sound module was connected to a Motu Microlite MIDI interface, which was in turn connected to an Acer laptop running Windows. This laptop presented the auditory stimuli and recorded the tapping data using custom-built software written in C++. Auditory stimuli were presented via over-ear scanner-compatible headphones, and tapping responses were collected via a custom built, fiberoptic laser light gate and converted to midi signal via an Arduino microcontroller (<https://www.arduino.cc>).

In the Virtual Partner task, participants were required to tap their finger in time with an adaptive auditory pacing sequence consisting of the four cowbell lead-in sounds followed by the 48 woodblock sounds.

Timing of the woodblock sounds was controlled by an algorithm that implemented phase correction, as in ADAM’s adaptation module (see section 2.4). Sequence inter-stimulus intervals were thus adjusted in a manner that compensated for a proportion of each asynchrony between participant taps and virtual partner pacing sounds. Specifically, the onset time of the next pacing sound was determined by calculating the most recent tap-to-tone asynchrony, multiplying it by the relevant phase correction parameter value, and adding the result to the virtual partner timekeeper period (which dictated its base tempo) to obtain the current sequence inter-stimulus interval (e.g., Fairhurst et al., 2013; Mills et al., 2015; Repp and Keller, 2008). The timekeeper period was set at 500 ms and three phase correction values were employed to produce different of virtual partner adaptivity: 0 (a non-adaptive metronome), 0.4 (moderate adaptivity), or 0.9 (high adaptivity). The cowbell lead-in inter-stimulus intervals were fixed at 500 ms while the ensuing inter-stimulus intervals between the 48 woodblock sounds varied according to the level of adaptivity. Participants were instructed to synchronize their finger taps as accurately as possible with the virtual partner sounds whilst also maintaining the initial tempo set by the cowbell lead-in sequence.

In the Tempo Change task, participants synchronized finger taps with a sequence where the tempo varied gradually, as in expressive timed music (Pecenka et al., 2013; van der Steen et al., 2015a). The lead-in cowbell sounds at the start of each sequence were presented at a constant tempo, with inter-stimulus intervals fixed at 500 ms, and the tempo of the ensuing 48 woodblock sounds gradually accelerated and decelerated between inter-stimulus intervals of 400 ms and 600 ms within a sinusoidal envelope. The first two woodblock inter-stimulus intervals continued the lead-in tempo, after which the tempo variations took place across four cycles with acceleration and deceleration portions spanning five or seven sounds. Different cycle lengths were used to discourage participants from predicting upcoming tempo changes with a global timing strategy (i.e., counting the number of tones within each cycle), instead encouraging them to predict each upcoming interval actively based on the most recent stimulus events (i.e., local timing strategy). For this task, participants were instructed to tap in synchrony with the target stimulus sequence as accurately as possible.

On each trial for both tasks, participants were also visually presented with novel abstract objects that were projected onto a screen at the end of the scanner bore. The objects consisted of 11 images from a set of 36 blue ‘Fribbles’ with textured surfaces, which were obtained from the website of Michael J. Tarr at Carnegie Mellon University (<http://www.tarlab.org/>). A fixation cross was initially presented on the screen concurrently with the lead-in sequence. Target woodblock sounds were accompanied by alternating Fribble and fixation cross stimuli, with each visual stimulus presented for 1 s. Each sequence of Fribbles contained either one, two, three, or four 1-back repetitions. On single-task trials, participants were instructed to focus on the fixation cross throughout all trials, but to otherwise ignore the Fribble stimuli. On dual-task trials, participants were instructed to count the number of 1-back repetitions in the sequence of Fribbles. It was assumed that this secondary visual working memory task would increase cognitive load by introducing additional attentional demands (see Pecenka et al., 2013). On dual-task trials, participants were prompted to indicate the number of visual targets (i.e., 1-back repetitions) with a button press after performing difficulty rating for that trial.

2.4. Behavioral data analysis

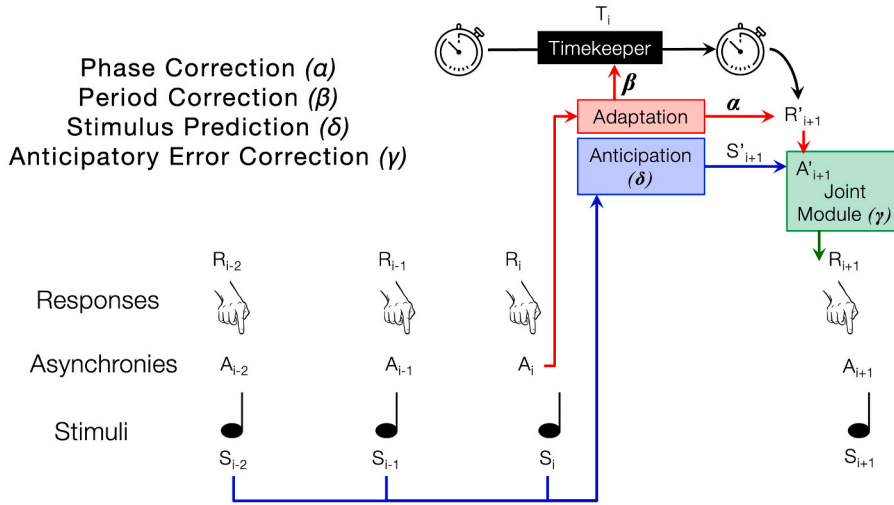
Behavioral data were screened to ensure suitability for model-based analysis with ADAM, as in earlier relevant studies (e.g., Mills et al., 2019; van der Steen et al., 2015a). Data analysis focused on the 4th to 47th event from the woodblock portion of each trial. Responses to preceding events were discarded to ensure that performance measures and modelling parameter estimates were not affected by unstable responses that can occur the initial segment of each trial. Trials with more

than five missing taps (pacing sounds without an accompanying response) or consecutive missing taps were rejected. Missing taps from the remaining trials were interpolated (Mills et al., 2019; Mills et al., 2015; van der Steen et al., 2015a). The quality of sensorimotor synchronization performance was assessed by computing the temporal asynchrony between stimulus events and corresponding tap responses in each trial (i.e., pacing event onset times were subtracted from tap times, resulting in negative asynchronies if taps preceded pacing sounds). Mean asynchrony was calculated as a measure of synchronization accuracy and the standard deviation of the asynchronies was used as a measure of synchronization variability (i.e., an inverse index of

synchronization stability). Inter-stimulus (tone onset) intervals and inter-response (tap) intervals were also computed for use as input in the ADAM parameter estimation procedure.

Individual differences in sensory-motor mechanisms and cognitive processes underlying task performance were assessed via a model-fitting parameter estimation procedure using ADAM (van der Steen et al., 2015a; van der Steen and Keller, 2013; van der Steen et al., 2015b). ADAM extends linear auto-regressive models of sensorimotor synchronization (Mates, 1994a, 1994b; Repp and Keller, 2004; Schulze et al., 2005; Vorberg and Schulze, 2002; Vorberg and Wing, 1996) by incorporating anticipatory processes, resulting in a model architecture with

A. Adaptation & Anticipation Model (ADAM)



B. ADAM Equations

$$s_i = S_i - S_{i-1} \quad (1)$$

$$r_i = R_i - R_{i-1} \quad (2)$$

$$A_i = R_i - S_i \quad (3)$$

Adaptation Module

$$R'_{i+1} = R_i + T_i - \alpha \times A_i + nT_i \quad (4)$$

$$T_i = T_{i-1} - \beta \times A_i \quad (5)$$

Anticipation Module

$$S'_{i+1} = S_i + \delta \times e_{i+1} + (1 - \delta) \times p_{i+1} + nT_i \quad (6)$$

$$e_{i+1} = 2 \times s_i - s_{i-1} \quad (7)$$

$$p_{i+1} = s_i \quad (8)$$

Joint Module

$$A'_{i+1} = R'_{i+1} - S'_{i+1} \quad (9)$$

$$R_{i+1} = R'_{i+1} - \gamma \times A'_{i+1} + nM_{i+1} - nM_i \quad (10)$$

Fig. 2. Formal components of the ADAM framework. A) Process diagram showing the relationship between stimuli (S), responses (R), and asynchronies between stimuli and responses (A). Tap response timing (e.g., R_{i+1}) is computed based on previous stimuli, responses, an internal timekeeper, and compensatory mechanisms within the adaptation, anticipation, and joint modules. Phase correction (α) and period correction (β) in the adaptation module generate action plans for timing the next response (R'_{i+1}). The weighting (δ) of extrapolation and perseveration processes in the anticipation module generate temporal predictions about the timing of the next sequence tone (S'_{i+1}). Anticipatory error correction (γ) in the joint module reduces discrepancies between plans and predictions before a motor command is issued and the response is executed (R_{i+1}). B) Equations for computing inter-stimulus (tone onset) intervals (1), inter-response (tap) intervals (2), and asynchronies (3) from behavioral data, which serve as input to equations for ADAM's adaptation module (4 & 5), anticipation module (6–8), and joint module (9 & 10) used in parameter estimation. S, stimulus (tone) onset; R, response (tap) onset; s, inter-stimulus interval, r, inter-response interval, A, asynchrony, T, timekeeper interval; R', planned response onset; S', predicted stimulus onset; A', anticipated error; e, extrapolated stimulus interval; p, perseverated stimulus interval; nT, timekeeper noise; nM, motor noise; α , phase correction, β , period correction; δ , prediction/tracking weight; γ , anticipatory error correction. Figure adapted from Harry and Keller (2019).

three computational modules: ‘adaptation’, ‘anticipation’, and ‘joint.’ The conceptual architecture of ADAM was shown in Fig. 1A and a process diagram showing the operation of the model is displayed in Fig. 2A. Equations for calculating timing measures are provided in Fig. 2B (Equations (1)–(3)), along with equations for each of ADAM’s modules (Equations (4)–(10); for further details, see Harry and Keller, 2019).

The adaptation module is used to estimate the gain of reactive error correction processes consisting of phase correction (α) and/or period correction (β). The anticipation module is used to estimate the strength of temporal predictions that are assumed to be based on the weighted sum of two processes, one entailing linear extrapolation of previous inter-stimulus intervals in the pacing sequence and the other copying the previous interval (controlled by the parameter δ). The joint module estimates the gain of an anticipatory error correction process (γ) that compensates for discrepancies between the outputs of the adaptation and anticipation modules. It is assumed that the joint module represents a process whereby potential temporal mismatches between action plans in ‘self’ internal models and predictions in ‘other’ internal models are reduced by adjusting one’s own plan prior to action execution. The anticipatory error correction parameter thus represents the balance of self-other integration and segregation. ADAM also includes two sources of noise, one that represents variability in a ‘timekeeper’ that is assumed to be instantiated in the central nervous system and the other representing ‘motor’ noise in the peripheral nervous system.

Estimates of performance-based ADAM parameter values were derived for individual participants by fitting the adaptation module or the full model to behavioral data for each trial in each task condition. Previous work using computer simulations (Harry and Keller, 2019) indicates that stimulus sequences with a roughly steady tempo, such as those from the Virtual Partner task, are best fit with ADAM’s adaptation module, which provides estimates of phase correction (α) and period correction (β), whereas sequences with gradual larger-scale variations in tempo, such as in the Tempo Change task, are best fit by including period correction (β), stimulus prediction (δ), and anticipatory error correction (γ) parameters from the full model. These two versions of ADAM (adaptation only or the full model) were fit to the behavioral data using a bounded Generalized Least Squares method (Jacoby and Repp, 2012; Repp et al., 2012; van der Steen et al., 2015a), which applies matrix algebra to inter-stimulus, inter-response, and asynchrony time series data (see Jacoby et al., 2015). Timekeeper noise was also estimated for each task in order to partial out random variability in the internal timekeeping mechanism that is assumed to be acted upon by the other processes. Complete details of the parameter estimation procedure can be found in Appendix A of the paper by van der Steen et al. (2015a).

Performance measures and model parameters were averaged over all trials from each of the two tasks in the two cognitive load conditions for each participant. In the Virtual Partner task, performance measures were averaged over virtual partner adaptivity levels (non-adaptive, moderate adaptivity, and high adaptivity) to derive a single performance estimate for each participant and cognitive load condition. Note that the non-adaptive condition (in which phase correction was set to 0 in the virtual partner) is essentially a steady tempo metronome as used in conventional sensorimotor synchronization experiments. Including the additional (non-zero) adaptivity conditions allowed us to examine processes that are likely to generalize to conditions that might be encountered in instances of coordination with real human partners. Collapsing across the three levels of adaptivity in our analyses was motivated by the current research aim focusing on individual differences rather than effects of this experimental manipulation.

2.5. MRI scanning & image processing

Imaging was conducted on a General Electric 3 T MRI. Echo planar T2*-weighted functional images were acquired with repetition time = 3 s, echo time = 32 ms, flip angle = 90, 47 axial slices covering the whole brain and cerebellum, field of view = 220 mm, and raw voxel size =

3.93.94 mm thick. Each functional scanning run comprised 117 volumes with an additional 8 volumes acquired to allow for equilibration effects (automatically discarded). High-resolution 3D T1-weighted, anatomical images (voxel size 0.40.40.9 mm) were obtained for co-registration with EPI data.

Dicom images were converted to nifti format via dcm2nii, and organized according to the BIDS format. Image pre-processing was carried out with fMRIPrep (v1.0.0-rc11). Anatomical pre-processing comprised skull stripping with ANTS, tissue segmentation with FSL-FAST, and spatial normalization to the MNI152NLin2009cAsym template using ANTS. Functional image pre-processing comprised FSL-MCFLIRT boundary-based motion correction, slice timing correction using AFNI-3dTShift, registration to the anatomical image with FSL-FLIRT and resampling to the template image.

Mean timeseries for 355 regions of interest were extracted for each task with Nilearn. Regions of interest for the cortex were defined by the Schaefer et al. (2018) MNI atlas comprising 300 parcels assigned to 17 networks, the Diedrichsen et al. (2009) 28 parcel cerebellar atlas, the 7 parcel Oxford Thalamic connectivity atlas, and the 7 parcel Oxford-GSK-Imanova striatal connectivity atlas (Fig. S1). Parcels in different hemispheres of the thalamic and striatal atlases were separated, increasing the parcel number to 14 for each structure. The time courses for cortical regions that corresponded to the visual canonical resting-state network in the Schaefer atlas were discarded, as visual responses were deemed not directly relevant to the audio-motor primary task used to probe the ADAM of sensorimotor synchronization.

2.6. Estimation of functional connectivity matrix

Functional connectivity matrices were obtained via correlational psychophysiological interactions analysis (cPPI), a method for obtaining estimates of task-modulated functional connectivity. Unlike traditional PPI, cPPI estimates the partial correlation between the task-modulated time courses of two regions to yield a single, symmetrical estimate of connectivity. A first-level model was estimated in SPM for each task and participant to provide regressors for task blocks, initial warning tones, post-trial responses, and a regressor to account for task blocks removed from the analysis either due to excessive movement (framewise displacement exceeding 0.3 mm during the block) or performance errors. In addition, confound regressors generated in the pre-processing stage comprising 6-rigid body parameters, framewise displacement, and 6 white and cerebral-spinal fluid time courses obtained via the aCompCor procedure were included in the estimation of functional connectivity. BOLD time courses extracted for Task modulated changes in functional connectivity were estimated for all pairs of regions via the cPPI toolbox.

2.7. Connectome-based predictive modelling

Connectome-based predictive modelling (CPM) was used to identify the brain networks associated with parameter estimates from the adaptation, anticipation, and joint modules of ADAM (Figs. 1A & 2). This technique identifies networks associated with sensory-motor and cognitive mechanisms by measuring brain-behavior relationships between task-evoked functional connectivity strength and task performance (Finn et al., 2015; Shen et al., 2017). The approach allows changes of functional connectivity among regions within the same brain network and between regions in different networks to be quantified. Within-network connectivity reflects the modulation of connections among nodes within a resting-state network in relation to individual differences in the process in question (here phase correction, period correction, stimulus prediction, or anticipatory correction), whereas between-network connectivity reflects the modulation of connections between nodes in different resting-state networks in relation to these processes. CPM has been shown to produce highly reproducible networks for examining individual differences (Taxali et al., 2021).

For each participant and task, we extracted BOLD timecourses from 300 cortical parcels derived from a resting-state cortical parcellation (Schaefer et al., 2018) (Fig. S1) and 55 sub-cortical parcels derived from the Oxford thalamic connectivity atlas (Behrens et al., 2003; Behrens et al., 2003), the Oxford-GSK-Imanova connectivity striatal atlas (Tziortzi et al., 2014), and the probabilistic cerebellar structural atlas (Diedrichsen et al., 2009). As connectivity with visual cortical regions was not expected to reflect individual differences in SMS task performance, regions corresponding to the visual resting-state network were omitted from analysis. Functional connectivity matrices that quantified the task-evoked changes in connectivity strength (task vs rest) between the remaining 315 cortical and subcortical regions were quantified with cPPI (Fornito et al., 2012). The networks associated with each behavioral parameter were identified by correlating individual differences in the behavioral parameter of interest with differences in connectivity strength of each element in the connectivity matrix. All connections (edges) showing a statistically significant ($P < 0.05$) relationship with the parameter of interest were included in the connectome-based predictive model, producing a network of edges positively correlated with the parameter ('high network') and a network of edges negatively correlated with the parameter ('low network'). Brain areas associated with the high network for a particular ADAM parameter (e.g., period correction) are more strongly connected in those individuals who exhibit high values on that parameter (i.e., engage in greater period correction), whereas regions in the corresponding low network are more strongly connected with low parameter estimates (i.e., stronger functional connectivity with less period correction).

Assessment of the networks identified by CPM proceeded via a two-stage procedure involving cross-validation followed by cross-task analysis. The first analysis stage tested the stability of the identified networks by applying a cross-validation procedure to examine whether the models derived from the single-task condition could be used to predict participants' behavioral parameter estimates from held-out brain-imaging data collected in the dual-task condition (and vice versa) for the Virtual Partner task and the Tempo Change task. Here, the strength of the network associated with the parameter of interest—phase correction for the Virtual Partner task and period correction, stimulus prediction, and anticipatory error correction for the Tempo Change task—was calculated for each participant as the sum of all connections identified in the edge-wise procedure described above. Separate network strength values were calculated for the high and low networks and incorporated in a GLM to model the relationship between network strength and the parameter of interest. The effects of each ADAM parameter of interest were partialled out from all other parameters using the procedure recommended by Shen et al. (2017). Then high and low network strength values were calculated from functional connectivity data obtained from the held-out condition and entered into the network strength model to derive estimates of the behavioral parameters. These brain-derived predicted measures of behavior were subsequently compared to behavior-derived model estimates with Spearman rank correlations to assess reliability of the identified network (Rosenberg et al., 2017; Shen et al., 2017).

Since all networks generalized across cognitive load conditions to some degree (see section 3.3), cross-task CPM was used to improve the reliability of the estimated network by incorporating both single and dual task conditions within a single model. Accordingly, each network was identified with the same edge-wise procedure as described above, however, here the design matrix used to examine the relationship between connection strength and model parameters also included dummy coded regressors for individual participants and the cognitive load conditions. The networks associated with the cross-task predictive model were characterized by identifying the prominent hubs, defined as nodes in the top 80th percentile for connectivity degree (Bertolero, Yeo, & D'Esposito, 2017) associated with low and high levels for each ADAM parameter. Hubs observed in the cerebral cortex were grouped into the seven canonical resting-state networks (control; default mode; dorsal

attention; salience/ventral attention; somatomotor; limbic frontal & temporal; temporal parietal) applied in the Schaefer et al. (2018) cortical parcellation (300 region), whereas hubs observed outside the cortex were grouped according to the relevant subcortical region (basal ganglia, thalamus, or cerebellum). As participants were engaged in an audio-motor primary task, it is worth noting that the ventral somatomotor network includes primary auditory cortex.

Permutation tests were carried out to assist in characterizing the composition of the networks identified by CPM. Firstly, permutation tests were used to identify cortical resting-state and subcortical networks that were observed to have a higher number of hubs than would be expected if hubs were randomly assigned to the cortical resting-state and subcortical networks. These tests involved randomly assigning regions to each of the 10 networks of interest (without replacement) and counting the number of hubs observed for 1000 permutations. The proportion of permutations where there were more hubs in a network than the empirical number of hubs was calculated and submitted to Benjamini-Hochberg False Discovery Rate correction ($q < 0.05$). Secondly, permutation tests were also carried out to identify high concentrations of connections within and between the 10 networks of interest. Permutation testing involved randomly assigning each of the 315 parcels to one of the 10 networks of interest (without replacement) and calculating the number of connections observed within and between the cortical resting-state and subcortical networks. The proportion of permutations where there were more connections within or between networks than the empirical number of connections was calculated and submitted to Benjamini-Hochberg False Discovery Rate correction ($q < 0.05$).

2.8. Assessing attentional modulation of network connectivity

Effects of attentional demands on ADAM networks were examined separately for the Virtual Partner task and the Tempo Change task. The complete CPM network was constructed separately for the Virtual Partner task (including only the phase correction network) and the Tempo Change task (including period correction, stimulus prediction, and anticipatory correction networks) and the sign of the connection (whether the connection was part of the high or low network) was ignored. These connections were grouped by the canonical networks (resting-state or subcortical structure) that they implicated. The strength of each of these canonical networks was calculated for each participant and cognitive load condition (single task or dual task) and entered into paired samples t-tests to examine the effect of cognitive load (single task > dual task). These cognitive load comparisons were computed for all within and between canonical network interactions (168 in total) and the Benjamini-Hochberg false correction procedure ($q < 0.05$) was applied to control false positive rate. The proportion of connections that corresponded to each of the ADAM networks identified by CPM was calculated for each canonical group of connections that was found to be modulated by the cognitive load manipulation to assess the extent to which attentional demands affected each of the ADAM networks.

3. Results

3.1. Behavioral analyses and model parameter estimation

Behavioral analyses were conducted (1) to confirm the effectiveness of cognitive load manipulation, and (2) to check the assumption that individual estimates of ADAM parameters account for individual differences in sensorimotor synchronization performance.

Descriptive statistics for the behavioral measures of synchronization accuracy (mean asynchrony) and variability (standard deviation of asynchronies) are shown in Fig. 3. Results are presented for a final participant sample of $n = 63$ in the Virtual Partner task and $n = 57$ in the Tempo Change task, after excluding participants with fewer than three valid trials per condition (due to head movement or excessive missing

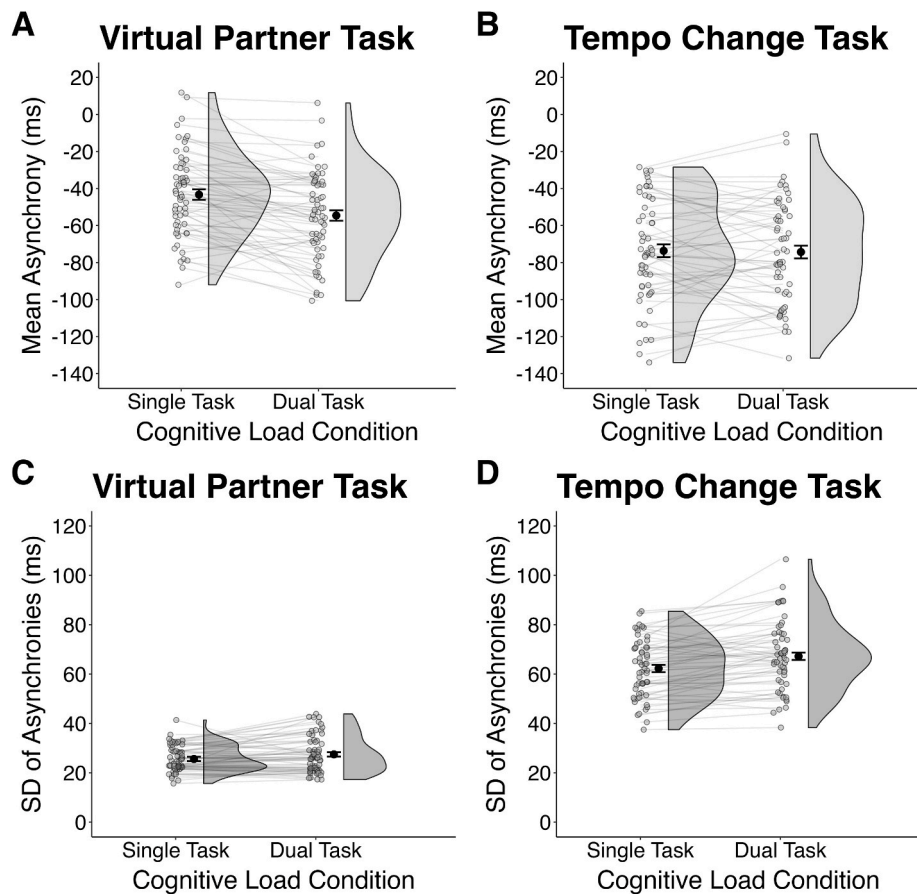


Fig. 3. Behavioral measures of sensorimotor synchronization accuracy (mean asynchrony) and stability (SD of asynchronies, an inverse measure) for the Virtual Partner (A–C) and Tempo Change (D–G) sensorimotor synchronization tasks under single-task and dual-task cognitive load conditions. Markers between density plots and individual data points represent sample averages for each measure and error bars indicate within-participants 95% confidence intervals.

taps; see section 2.4). Preliminary analyses indicated that the accuracy and variability of asynchronies did not differ between participants with and without musical training (Fig. S2 & Table S2), and therefore we did not include musical experience as a factor in the main analyses. A possible reason for the lack of an effect of musical experience on these behavioral measures is that all participants had participated in previous sensorimotor synchronization experiments using similar tasks (including a behavioral session of the procedure a week before scanning), and hence can be viewed as having task-specific experience.

In the main analyses, paired samples t-tests comparing performance in the single-task and dual-task conditions in the Virtual Partner task revealed that synchronization accuracy and stability were impaired when participants were required to do the secondary visual working memory task. Mean asynchrony (Fig. 3A) was generally negative—indicating that taps preceded pacing sounds, as is typical in sensorimotor synchronization tasks (Repp, 2005)—but significantly more so in the dual-task than the single-task condition ($T_{62} = 5.67$, $P < 0.001$). The standard deviation of asynchronies (Fig. 3C) was significantly higher, indicating less stable synchronization, in the dual-task than the single-task condition ($T_{62} = -2.67$, $P = 0.01$). For the Tempo Change task, mean asynchrony (Fig. 3B) did not differ significantly across single-task and dual-task conditions ($T_{56} = -0.277$, $P > 0.7$), but the standard deviation of asynchronies (Fig. 3D) was significantly higher in the dual-task condition ($T_{56} = -4.72$, $P < 0.001$). These results indicate that synchronization stability was more sensitive than synchronization accuracy to the manipulation of cognitive load.

ADAM parameter estimates derived from the Virtual Partner and Tempo Change tasks are shown in Fig. 4. Paired samples t-tests comparing model estimates in the single-task and dual-task conditions

confirmed that the visual working memory task affected values for most parameters. For the Virtual Partner task (Fig. 4A–C), phase correction ($T_{62} = -2.53$, $P = 0.014$), period correction ($T_{62} = -2.93$, $P = 0.005$), and timekeeper noise ($T_{62} = -4.79$, $P < 0.001$) were significantly higher in the dual-task condition compared to the single-task condition. These results suggest that increases in the variability of an internal time-keeping processes induced by the secondary task were compensated for (albeit only partially, given the results for synchronization accuracy and stability) by slight increases in the gain of phase correction and period correction (see Repp et al., 2012). Although period correction was assumed not to be necessary due to the regular tempo in Virtual Partner task, previous work has found that it can nevertheless be recruited when task difficulty increases (Repp and Keller, 2008).

For the Tempo Change task (Fig. 4D–G), as expected, period correction ($T_{56} = 4.88$, $P < 0.001$) and anticipatory error correction ($T_{56} = 9.65$, $P < 0.001$) were significantly lower in the dual-task condition compared to the single-task condition. Neither timekeeper noise ($T_{56} = -0.98$) nor stimulus prediction ($T_{56} = -0.29$) showed a significant difference between the single-task and dual-task conditions. The lack of a reliable difference for timekeeper noise may be attributable to a ceiling effect due to the generally high levels of variability created by the constant need to adjust the timekeeper period, as well as the overshoot at reversal points between accelerating and decelerating sections of the sequences (Mills et al., 2019; van der Steen et al., 2015a). The lack of an effect for stimulus prediction is likely related to participants displaying a wide range of values for this parameter, with a slight overall tendency to track the tempo changes (indicated by average parameter estimate values being less than 0.5), which is an automatic process that is relatively resistant to dual-task interference (Pecenka et al., 2013).

Virtual Partner Task

Tempo Change Task

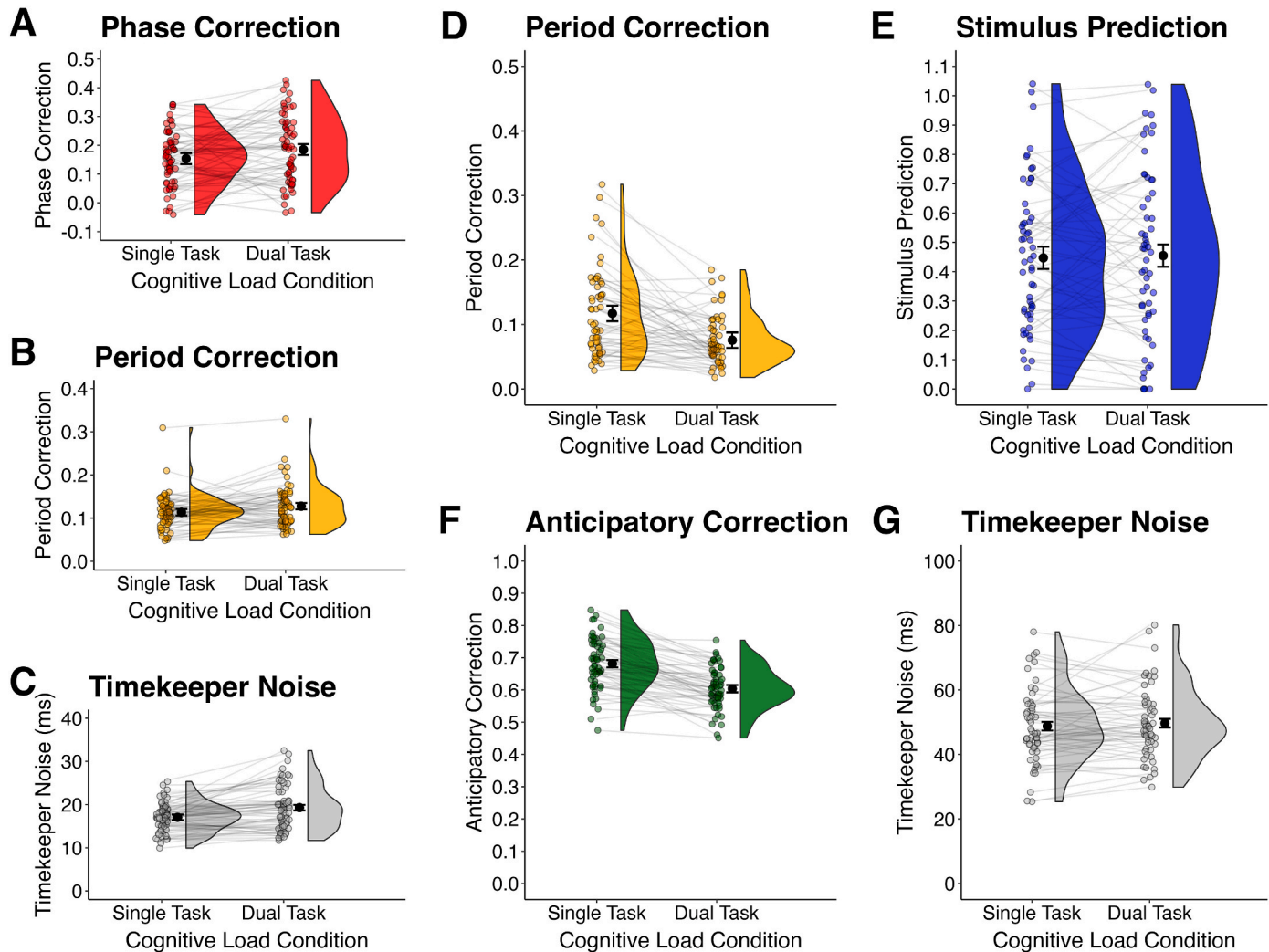


Fig. 4. ADAM parameter estimates for the two sensorimotor synchronization tasks under single-task and dual-task cognitive load conditions. Different versions of the model were used for Virtual Partner (A–C) and Tempo Change (D–G) tasks. Phase correction and period correction relate to ADAM's adaptation module, stimulus prediction relates to the anticipation module, and anticipatory error correction relates to the joint module. Markers between density plots and individual data points represent sample averages for each measure and error bars indicate within-participants 95% confidence intervals.

To assess the contribution of each ADAM parameter to behavioral performance, we examined how the variability in parameter estimates across participants was related to individual differences in synchronization accuracy and stability using mixed effects linear regression implemented by the lme4 package (version 1.1–30) in R (version 4.2.1). ADAM parameter estimates and cognitive load condition were included as fixed effects and participant was included as a random effect (See Tables S3–S6 in the Supplementary Materials for details of the analyses, and Tables S7–S8 for tests of collinearity among fixed effects.). While there was little evidence for reliable relationships with synchronization accuracy (mean asynchrony) (Fig. S3 & Tables S3–S4), model parameters accounted well for synchronization variability (standard deviation of asynchronies), as described below (Fig. 5 & Tables S5–S6). The less robust results for synchronization accuracy are consistent with previous computer simulations (Harry and Keller, 2019) and proposals that the negative mean asynchrony is a combined consequence of sensory-motor processing delays, biases in time interval perception, and timekeeper detuning or miscalibration (Repp, 2005).

For the Virtual Partner task (Fig. 5A–C), the variability of asynchronies was significantly related to phase correction (negative

relationship, Effect Estimate = -9.94 , $SE = 3.19$, $T = -3.12$, 95% $CI [-16.26, -3.61]$), period correction (negative relationship, Estimate = -17.84 , $SE = 7.49$, $T = -2.38$, $CI [-32.72, -2.99]$), and timekeeper noise (positive relationship, Estimate = 1.30 , $SE = 0.09$, $T = 14.82$, $CI [1.13, 1.48]$). In other words, unstable synchronization was associated with low phase correction, low period correction, and high timekeeper noise. A reduced linear model that included only the random effect was also tested to evaluate the explanatory power of the full model via model comparison. A likelihood-ratio test indicated that the full model including ADAM parameter estimates and cognitive load condition provided a better fit to the data than the reduced model ($\chi^2(7) = 221.63$, $P < 0.001$; Log Likelihood = -283.61 (full) vs -394.43 (reduced), AIC = 587.23 vs 794.86 , BIC = 615.59 vs 803.36).

For the Tempo Change task (Fig. 5D–G), variability of asynchronies was significantly related to period correction (positive relationship, Estimate = 20.57 , $SE = 8.98$, $T = 2.29$, $CI [2.79, 38.37]$), stimulus prediction (negative relationship, Estimate = -28.41 , $SE = 1.98$, $T = -14.34$, $CI [-32.57, -24.18]$), anticipatory error correction (negative relationship, Estimate = -83.94 , $SE = 8.08$, $T = -10.83$, $CI [-99.94, -67.87]$), and timekeeper noise (positive relationship, Estimate = 0.62 ,

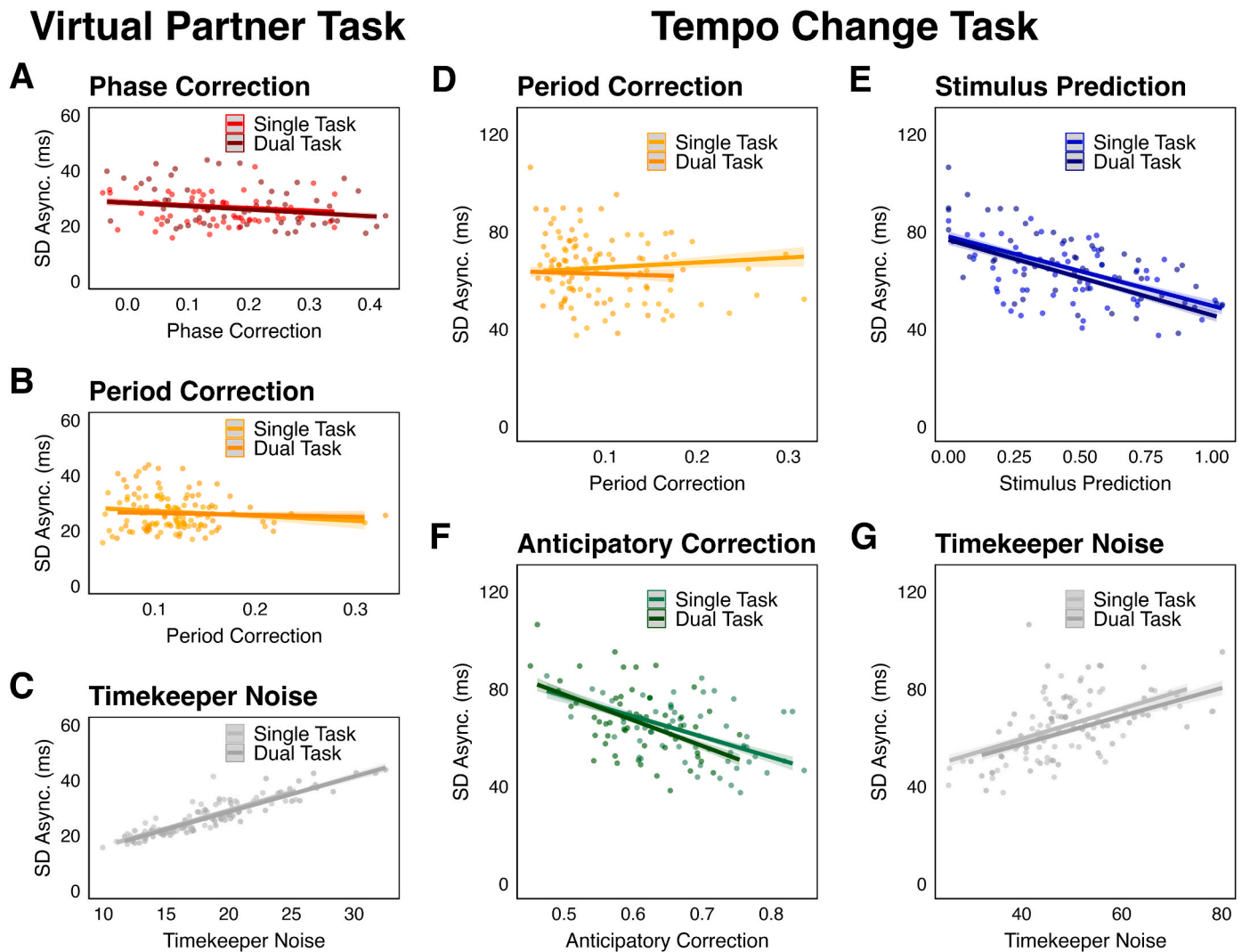


Fig. 5. Predictor effect plots showing relations between each ADAM parameter estimate and the stability of sensorimotor synchronization (SD of asynchronies, an inverse measure) revealed by mixed effects linear regression analyses for the Virtual Partner (A–C) and Tempo Change (D–G) tasks. Data points are values for individual participants averaged separately in the single-task and dual-task cognitive load conditions. Plots of partial residuals can be found in Fig. S4.

$SE = 0.04$, $T = 13.81$, $CI [0.52, 0.71]$). Unstable synchronization was thus associated with high period correction, low stimulus prediction, low anticipatory error correction, and high timekeeper noise. A likelihood-ratio test indicated that the full model provided a better fit to the data than the reduced model including only the random effect ($\chi^2(9) = 248.95$, $P < 0.001$; Log Likelihood = -307.07 (full) vs -431.53 (reduced), AIC = 638.10 vs 869.05 , BIC = 670.94 vs 877.26).

3.2. Brain network identification

CPM was used to identify brain networks associated with ADAM's three modules by measuring relationships between task-evoked functional connectivity strength and ADAM parameter estimates. ADAM's adaptation module was identified based on phase correction estimates from the Virtual Partner task and period correction estimates from the Tempo Change task. The anticipation module was examined based on stimulus prediction estimates, while the joint module was addressed based on anticipatory error correction estimates from the Tempo Change task.

When applied to phase correction parameter estimates from the Virtual Partner task, the cross-validated CPM procedure identified networks in the single-task and dual-task conditions that could account for phase correction in the held-out dataset (single task to dual task cross

validation; $r_{61} = 0.37$, $P = 0.003$, dual task to single task cross validation; $r_{61} = 0.26$, $P = 0.043$). Cross-task CPM identified a phase correction network comprising 1736 connections positively correlated with phase correction parameter estimates (Table S9 & Fig. S5) and 529 connections negatively correlated with parameter estimates (Table S10 & Fig. S6). Fig. 6A shows the hubs associated with the high and low phase correction networks. The high phase correction network (colored red) consists of positive connections, indicating that stronger functional connectivity is associated with greater phase correction, while the low phase correction network (colored blue) consists of negative connections, reflecting stronger connectivity with less phase correction. Permutation tests revealed a larger number of hubs than would be expected by chance in several divisions of the high phase correction network (red), including the majority of the cerebellum, as well as regions that reside in the dorsal and ventral bilateral somatomotor, salience/ventral attention, and basal ganglia resting-state networks (Fig. 6B, red). The cortical hubs, which had prolific cross-network connections (Fig. 6C, red), included the insular, posterior medial frontal, pre-motor, and supramarginal gyrus. Hubs in the low phase correction network (blue) consisted of regions in the default mode, temporo-parietal, and limbic resting-state networks (Fig. 6B, blue), and were less richly interconnected (Fig. 6C, blue).

Networks associated with period correction parameter estimates in

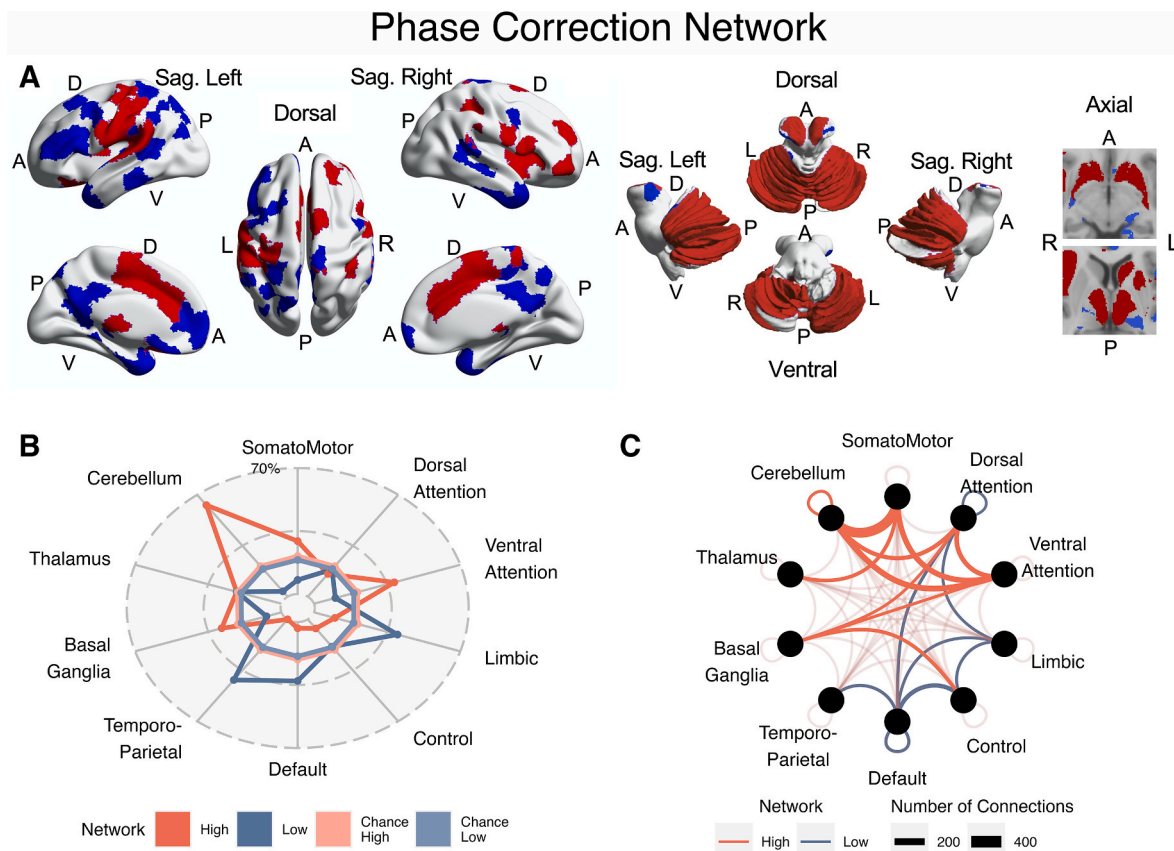


Fig. 6. High (red) and low (blue) networks associated with PHASE CORRECTION estimates related to the ADAM adaptation module. Functional connectivity within the high network increases with increasing phase correction while connectivity in the low network increases with decreasing phase correction. **A)** Hub nodes depicted on inflated cortical and cerebellar surfaces and volume images of the basal ganglia and thalamus with regions participating in both high and low networks shown in purple. **B)** Proportion of hub regions that reside in each cortical resting-state network (visual networks omitted) and subcortical structure with permutation derived chance proportion of hubs shown in pale colors. **C)** Number of connections formed within and between resting-state networks and subcortical structures for the high and low networks identified by CPM. Connections that are more numerous than is expected from permutation testing are shown in solid colors and connections that are not more numerous than is expected from permutation testing are transparent.

the Tempo Change task showed asymmetric cross-validation performance, with network strength from the dual task accounting for period correction estimates from the single task, but not vice versa (single task to dual task cross validation; $r_{55} = -0.007$, $P = 0.95$, dual task to single task cross validation; $r_{55} = 0.38$, $P = 0.004$). The cross-task predictive model comprised 3269 positive connections (Table S11 & Fig. S7) and 253 negative connections (Table S12 & Fig. S8). Positive connections form the high period correction network, in which stronger functional connectivity is associated with greater period correction, while negative connections form the low period correction network, where connectivity is stronger with less period correction.

Permutation tests revealed a large concentration of hubs (Fig. 7A, red) in the temporo-parietal, default mode, and somatomotor resting-state networks, as well as cerebellar, basal ganglia, and thalamic networks for the high period correction network (Fig. 7B, red). The majority of connections observed in the high period correction network were located within and between somatomotor and default mode networks (Fig. 7C, red), though the default mode network was also richly connected with the salience/ventral attention, control, and basal ganglia networks. Permutation tests did not reveal a particularly large concentration of hubs in any of the 10 networks of interest for the low period correction network. Nevertheless, the number of hubs in the salience/ventral attention, limbic (frontal), control, and default mode resting-state networks (Fig. 7A, blue) was greater than expected by chance (Fig. 7B, blue), with the majority of connections observed within the default mode network and between control and ventral attention networks (Fig. 7C, blue).

Networks associated with the parameter estimates for stimulus prediction revealed that each network accounted for stimulus prediction in the held-out dataset (single task to dual task cross validation; $r_{55} = 0.39$, $P = 0.003$, dual task to single task cross validation; $r_{55} = 0.35$, $P = 0.008$). Cross-task analysis identified a stimulus prediction network comprising 300 positive connections (Table S13 & Fig. S9) and 2740 negative connections (Table S14 & Fig. S10). Permutation tests revealed a high concentration of hubs (Fig. 8A, red) in the cerebellum, thalamus, and the control and limbic resting-state networks (Fig. 8B, red) in the high stimulus prediction network (extrapolation-based prediction), with the majority of connections observed between cerebellar, control, and somatomotor network regions (Fig. 8C, red). Hubs in the low stimulus prediction network (tracking-based prediction) predominantly reside in cerebellar and basal ganglia subcortical networks and the somatomotor and temporo-parietal resting-state networks (Fig. 8A & B, blue), with connections mainly between somatomotor and temporo-parietal networks and within somatomotor, cerebellar, basal ganglia, and thalamic networks (Fig. 8C, blue).

Cross-validation analysis of the anticipatory error correction networks revealed that the network strength models derived from the single and dual tasks generalize to anticipatory error correction parameter estimates from the corresponding held out task (single task to dual task cross validation; $r_{55} = 0.29$, $P = 0.029$, dual task to single task cross validation; $r_{55} = 0.26$, $P = 0.044$). Cross-task analysis identified an anticipatory error correction network comprising 2867 positive connections (Table S15 & Fig. S11) and 463 negative connections (Table S16 & Fig. S12). Permutation tests revealed a high concentration

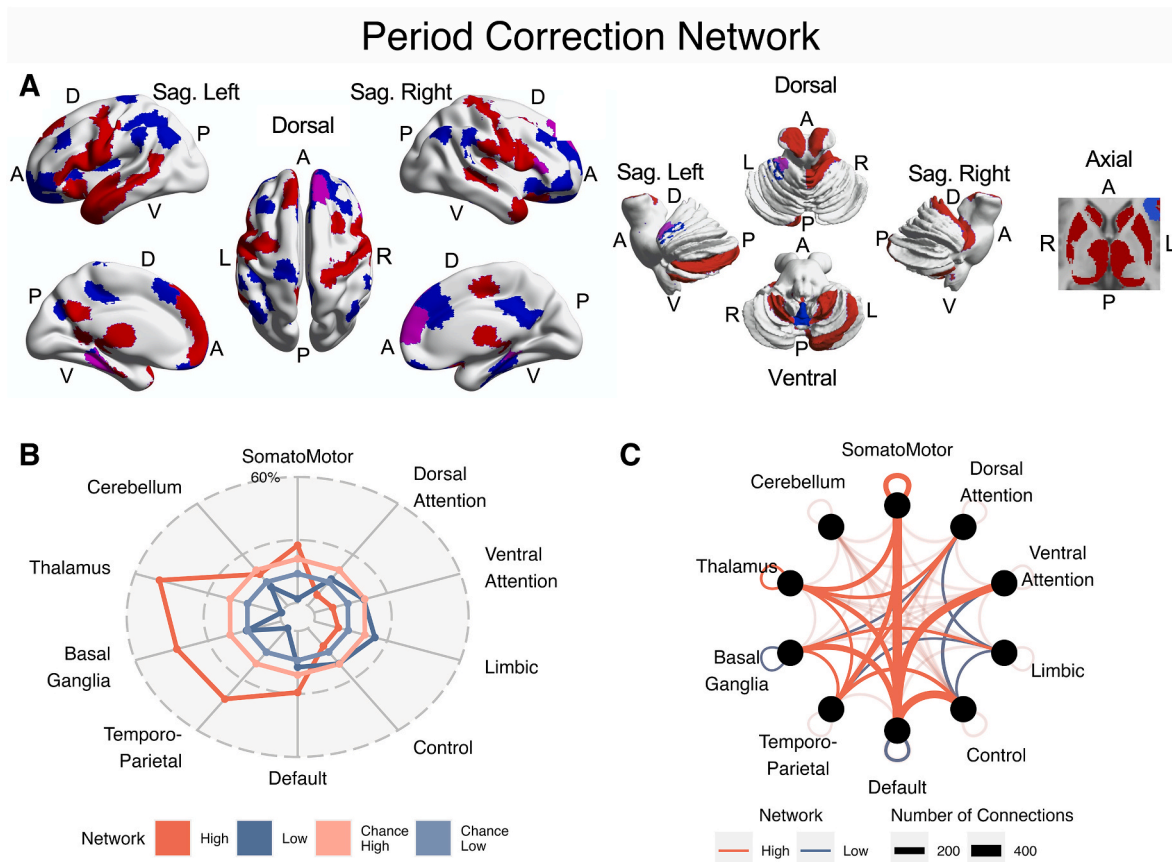


Fig. 7. High (red) and low (blue) networks associated with PERIOD CORRECTION estimates related to the ADAM adaptation module. **A)** Hub nodes depicted on inflated cortical and cerebellar surfaces and volume images of the basal ganglia and thalamus with regions participating in both high and low networks shown in purple. **B)** Proportion of hub regions that reside in each cortical resting-state network (visual networks omitted) and subcortical structure with permutation derived chance proportion of hubs shown in pale colors. **C)** Number of connections formed within and between resting-state networks and subcortical structures for the high and low networks. Connections that are more numerous than is expected from permutation testing are shown in solid colors and connections that are not more numerous than is expected from permutation testing are transparent.

of hubs (Fig. 9A red) in the default mode, temporo-parietal, and thalamic resting-state networks for the high anticipatory correction network (Fig. 9B, red), with the majority of connections observed within the default mode network and between regions in the default mode, control, salience/ventral attention, and somatomotor resting-state networks (Fig. 9C, red). Hubs in the low anticipatory error correction network predominantly reside in the salience/ventral attention and dorsal attention resting-state networks, as well as the basal ganglia (Fig. 9A & B, blue). For this network, the majority of connections were observed within ventral attention and dorsal attention networks and between control, basal ganglia, ventral attention, somatomotor, and cerebellar regions (Fig. 9C, blue).

The common brain regions identified across all networks were examined to reveal brain hubs forming a cluster that, analogously to a 'rich club' (van den Heuvel and Sporns, 2013), potentially combines and regulates information across the broader collective networks. Cross-network hubs were identified under two conditions; 1) for hubs identified across all four networks associated with the Virtual Partner task and the Tempo Change task, and 2) for hubs identified across the three networks associated with the Tempo Change task. Cross-network hubs that were identified in all four networks comprised ventral pre-/post-central gyrus, superior frontal gyrus, supplementary motor area, middle frontal gyrus, frontal pole, middle temporal gyrus, temporal pole, supramarginal gyrus, central opercular cortex, insular cortex, posterior cingulate, left precuneus, putamen, cerebellum left crus II, and thalamus. In addition to these regions, the cross-network hubs identified for the three networks observed in the Tempo Change task included

inferior frontal gyrus and superior temporal gyrus. These cross-network hubs are listed with associated resting-state networks in Table 1 and shown in Fig. 10.

3.3. Attentional modulation of network connectivity

To assess the influence of attentional demands on functional connectivity in the ADAM networks identified by CPM, we calculated the average connectivity within and between all the canonical resting-state networks and subcortical connections identified in all the predictive models (i.e., all connections identified across all ADAM parameters) for each participant and cognitive load condition, and compared these mean connectivity values across cognitive load conditions. For the Virtual Partner task, connectivity strength comparisons were derived only for phase correction, whereas in the Tempo Change task, all connections identified for period correction, stimulus prediction, and anticipatory error correction were examined together. Paired-samples t-tests were used to compare mean connectivity strength across the single and dual task conditions (single task > dual task) for all within- and between-resting-state connections, with the Benjamini-Hochberg false correction procedure ($q < 0.05$) applied to control the false discovery rate.

For the Virtual Partner task, there were no significant effects of the cognitive load manipulation on the connections related to phase correction. In contrast, for the Tempo Change task, a number of significant effects of cognitive load were observed for connections between control, default mode, and dorsal attention networks. Overall, the dual-task condition was associated with increased connectivity in

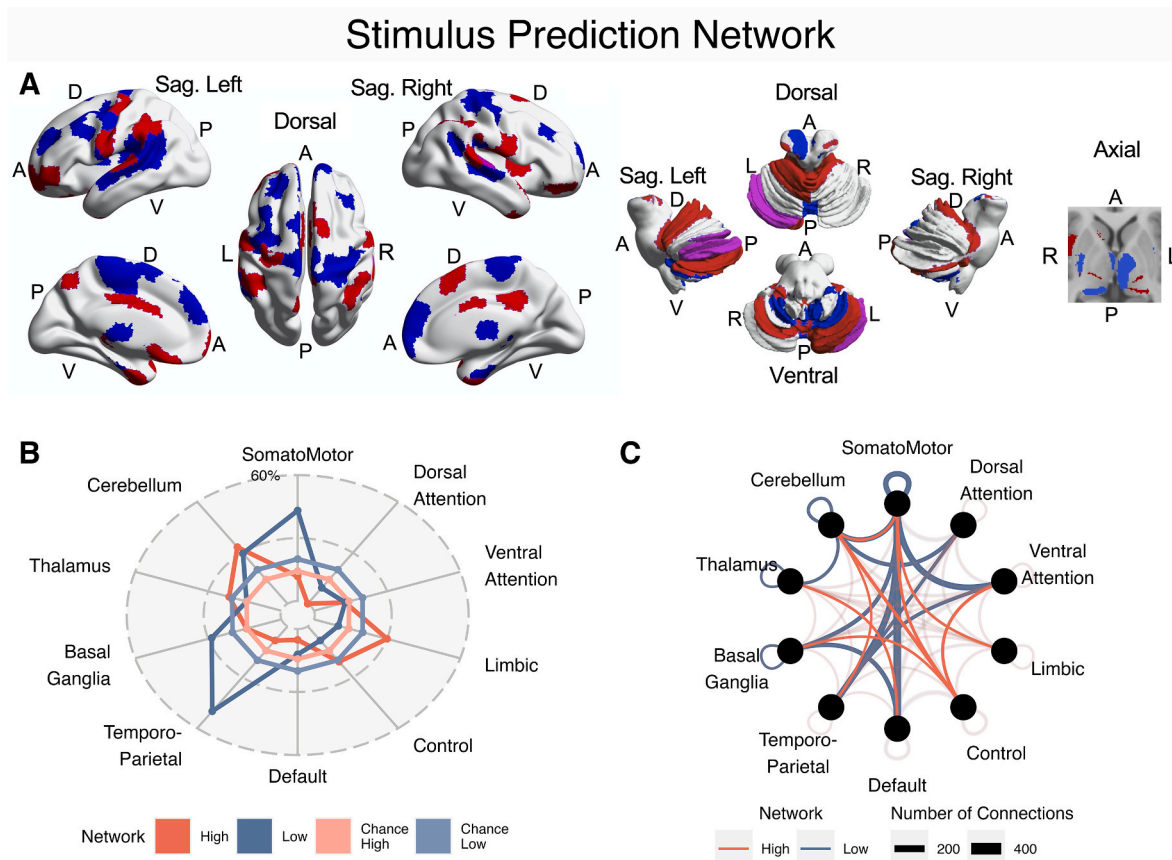


Fig. 8. High (red) and low (blue) networks associated with STIMULUS PREDICTION estimates related to the ADAM anticipation module. **A)** Hub nodes depicted on inflated cortical and cerebellar surfaces and volume images of the basal ganglia and thalamus with regions participating in both high and low networks shown in purple. **B)** Proportion of hub regions that reside in each cortical resting-state network (visual networks omitted) and subcortical structure with permutation derived chance proportion of hubs shown in pale colors. **C)** Number of connections formed within and between resting-state networks and subcortical structures for the high and low networks. Connections that are more numerous than is expected from permutation testing are shown in solid colors and connections that are not more numerous than is expected from permutation testing are transparent.

components of the ADAM network linked to control, default mode, and dorsal attention resting-state networks, and decreased connectivity within components of the ADAM network linked to the control resting-state network. To understand how the modulated connections relate to different components of the ADAM network, the modulated networks are shown overlaid on the networks for period correction, stimulus prediction, and anticipatory error correction in Fig. 11. Connections between control, default mode, and dorsal attention networks that were modulated by attention largely overlapped with connections observed in period correction and anticipatory error correction networks, a finding that is consistent with the behavioral results indicating that period correction and anticipatory error correction decreased under increased cognitive load in the Tempo Change task. In contrast, decreased connectivity was observed among regions within the control network under dual-task conditions compared to single-task conditions. These connections exclusively overlapped with the stimulus prediction network. The functional specificity of this result is uncertain given that behavioral stimulus prediction estimates were not affected by cognitive load.

Drawing together the results from the Virtual Partner and Tempo Change tasks, attentional modulation induced by the visual working memory task increased connectivity in networks associated with period correction, anticipatory error correction, and to a lesser extent stimulus prediction. There was no reliable evidence of attentional modulation of networks associated with phase correction. These results are consistent with previous findings showing that phase correction is an automatic process, whereas period correction and the other mechanisms associated with synchronization with tempo changes are modulated by attention

(Pecenka et al., 2013; Repp, 2005; Repp and Keller, 2004). A similar analysis comparing connectivity between single and dual task conditions in the Virtual Partner task for all connections identified across all CPM networks and related ADAM parameters (i.e., not just restricted to connections in the phase correction, period correction, and timekeeper noise) revealed widespread attentional modulation across control, default, dorsal attention, and ventral attention networks (Table 2). Notably, this analysis did not reveal modulation of connections between the somatomotor, ventral attention, and cerebellar networks, which were prominent connections identified in the CPM for phase correction (Fig. 6).

4. Discussion

The present study combined connectome-based predictive modelling (CPM) of fMRI data and computational modelling of sensorimotor synchronization behavior to identify brain networks that support temporal adaptation, anticipation, and the monitoring and integration of information about one's own actions and externally controlled auditory pacing sequences. Our analyses revealed variations in functional connectivity within and between distinct but overlapping brain networks that were associated with individual differences in parameter estimates reflecting processes instantiated in the adaptation and anticipation model (ADAM) of sensorimotor synchronization with regular and tempo-changing sequences (Harry and Keller, 2019; van der Steen and Keller, 2013). Cross-validation and comparison across conditions of low and high cognitive load demonstrated the reliability of, and stability in

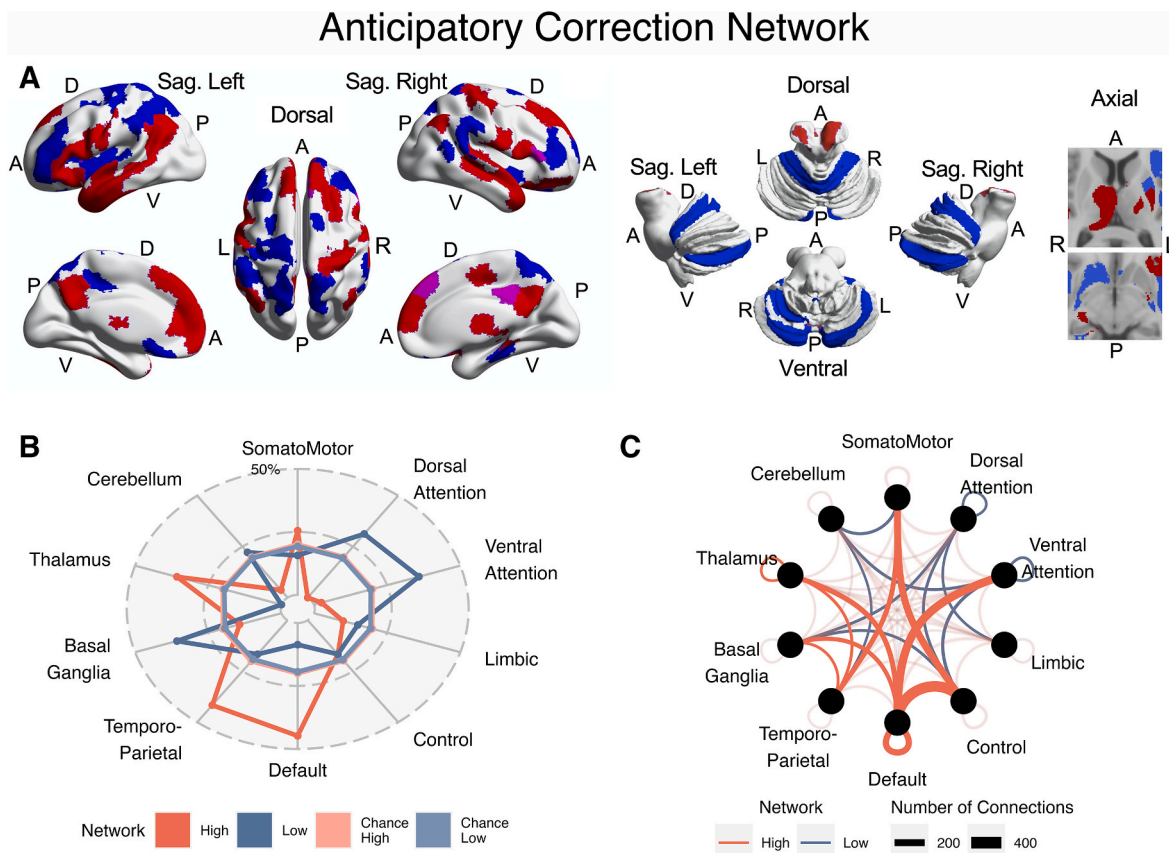


Fig. 9. High (red) and low (blue) networks associated with ANTICIPATORY ERROR CORRECTION estimates related to the ADAM joint module. **A)** Hub nodes depicted on inflated cortical and cerebellar surfaces and volume images of the basal ganglia and thalamus with regions participating in both high and low networks shown in purple. **B)** Proportion of hub regions that reside in each cortical resting-state network (visual networks omitted) and subcortical structure with permutation derived chance proportion of hubs shown in pale colors. **C)** Number of connections formed within and between resting-state networks and subcortical structures for the high and low networks. Connections that are more numerous than is expected from permutation testing are shown in solid colors and connections that are not more numerous than is expected from permutation testing are transparent.

global brain network structure accompanied by attention-related modulations of connectivity strength and hub configuration across networks linked to ADAM's adaptation, anticipation, and joint modules.

Overall results indicate that a core network of hub regions—a potential ADAM 'rich club' (Table 1 & Fig. 10)—modulates functional connectivity within and between the brain's resting-state networks and additional sensory-motor regions and subcortical structures in a manner that supports sensorimotor synchronization under conditions that differ in terms of tempo profile and concurrent cognitive demands (Fig. 12). This study thus contributes to efforts to understand how the functional organization of resting-state networks supports flexible cognition and behavior (Cohen & D'Esposito, 2016; Deco et al., 2015; Dixon et al., 2017; Sporns, 2013; Wang et al., 2021) by extension to the domain of real-time rhythmic coordination. In particular, our findings are informative about how brain network reconfiguration fulfills functions associated with different ADAM modules by (1) shifting focus on internal and external information, and (2) varying the degree of simultaneous integration and segregation of these different information sources.

4.1. Internal vs external focus in the adaptation & anticipation networks

A large body of research has shown that the reconfiguration of resting-state networks facilitates flexibility in shifting focus between internal and external information in order to fulfil diverse task demands (see Bassett and Sporns, 2017; Cole et al., 2014; Crossley et al., 2013). During sensorimotor synchronization, external focus on the pacing sequence and internal self-focus are associated with distinct neural

pathways that mediate beat finding (external) and beat keeping (internal) (Todd and Lee, 2015a). Our results reveal links between individual differences in the task-based functional connectivity of these pathways and the operation of fundamental mechanisms that support rhythmic coordination.

Individuals with relatively high phase correction had stronger connectivity between cingulo-opercular, cerebellar, and somatomotor regions (including auditory cortex) from the ventral attention and salience networks, whereas individuals with lower phase correction had stronger connectivity between midline default mode regions and right-lateralized frontal regions from the central executive control network. The regions within these networks are consistent with key regions identified in previous studies of auditory-motor coupling during sensorimotor synchronization (e.g., Bijsterbosch et al., 2011; Praamstra et al., 2003; Rao et al., 1997; Repp and Su, 2013; Stephan et al., 2002), as summarized in Table S1. Our findings extend this previous work by elucidating how individual differences in phase correction are related to the interplay of these regions within the brain's resting-state networks.

The distinction between high and low phase correction networks can be characterized a difference in the degree of external versus internal focus. Phase correction involves exogenously driven perceptual-motor coupling (Repp, 2005; Repp and Keller, 2004). Increased focus on internal performance monitoring can weaken such coupling by reducing the gain of phase correction (Fairhurst et al., 2014). Our results suggest that external focus is associated with strong functional connectivity within the ventral attention/salience regions in the high phase correction network (where connectivity increases with increasing phase correction), whereas internal focus is reflected in connectivity between

Table 1
Common brain regions associated with ADAM’s adaptation, anticipation, and joint networks, along with the resting-state network(s) to which they belong. Each of the main resting-state networks is represented by at least one common node, providing an exhaustive set of potential links for mediating information flow and network reconfiguration. * Appears only across the three networks associated with the Tempo Change task.

| ADAM common regions | Resting-State Network(s) |
|--|--|
| Cerebellum - crus-II (LH) | Cerebellar |
| Basal Ganglia - Occipital (LH) (Putamen) | Striatal (Basal Ganglia) |
| Thalamus - Temporal (LH/RH) | Thalamic |
| Posterior Cingulate Cortex (LH/RH) | Default; Control; Salience/VAN |
| Precuneus Cortex (LH) | Default; Control; Salience/VAN |
| Insular Cortex (RH) | Salience/VAN; SomatoMotor |
| Superior Temporal Gyrus – anterior (LH)* | Temporal-Parietal |
| Middle Temporal Gyrus – temporooccipital (LH) | Temporal-Parietal; Control |
| Middle Temporal Gyrus – posterior (RH) | Temporal-Parietal; Default; Control |
| Temporal Pole (LH/RH) | Default; Limbic; Temporal-Parietal |
| Postcentral Gyrus (LH/RH) – (Somatosensory cortex) | SomatoMotor; Salience/VAN; Dorsal Attention |
| Precentral Gyrus (LH/RH) – (Primary motor cortex) | SomatoMotor; Control; Salience/VAN; Dorsal Attention |
| Supplementary Motor Area (LH/RH) | SomatoMotor; Salience/VAN |
| Supramarginal Gyrus – anterior (LH) | Salience/VAN; Dorsal Attention |
| Supramarginal Gyrus - posterior (RH) | Salience/VAN; Control; Temporal-Parietal |
| Central Opercular Cortex (LH) | SomatoMotor; Salience/VAN |
| Inferior Frontal Gyrus - pars triangularis (LH)* | Default |
| Middle Frontal Gyrus (LH) | Control; Default; Control; Salience/VAN |
| Superior Frontal Gyrus (LH/RH) | Default; Salience/VAN; Control |
| Frontal Pole (LH/RH) | Control; Salience/VAN; Default; Limbic |

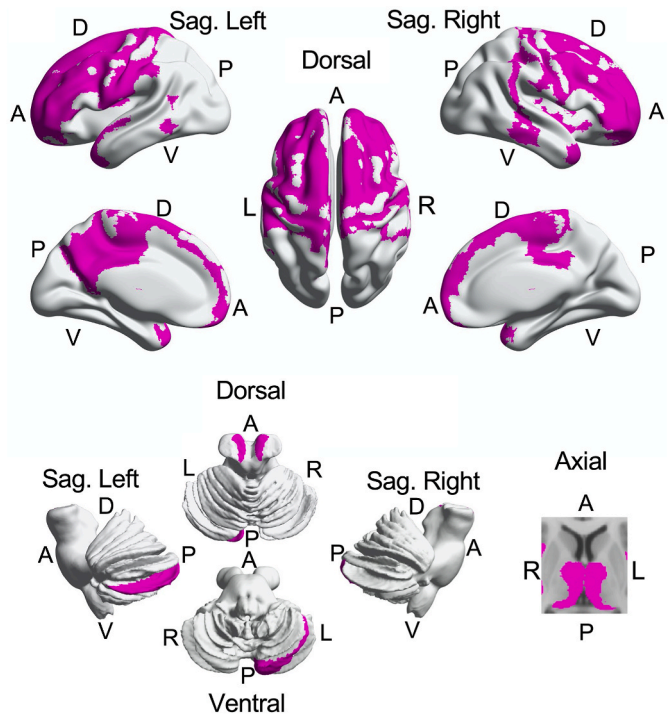


Fig. 10. Common ‘rich club’ brain regions associated with ADAM’s adaptation, anticipation, and joint networks depicted on inflated cortical and cerebellar surfaces and a volume image of the basal ganglia and thalamus.

default mode and control regions in the low phase correction network (where connectivity increases with decreasing phase correction). Previous experimental manipulations of the strength of auditory-motor coupling in various rhythmic contexts implicate similar networks (Fairhurst et al., 2013, 2014; Hove et al., 2016; Jasmin et al., 2016). The present study goes further by pinning variations in the interplay of these networks specifically to individual differences in phase correction and the quality of sensorimotor synchronization performance. While our study was not designed to compare the effects of different levels of Virtual Partner adaptivity (cf. Fairhurst et al., 2013, 2014), doing so in future research could determine how these individual differences affect coordination with partners who vary in ‘cooperativity.’

In contrast to phase correction, period correction entails cognitively mediated adjustments to the base interval (or oscillatory frequency) of an endogenous timekeeper that drives movement (Repp and Keller, 2004) and hence can be assumed to benefit from internal focus. Previous work has emphasized the role of subcortical sensorimotor regions in instantiating endogenous timekeepers that interact with cortical regions involved in monitoring the alignment of one’s own action timing and the external pacing events, and in evaluating the temporal mismatch between them (Bijsterbosch et al., 2011; Grahn and Rowe, 2013; Levitin et al., 2018; Repp and Su, 2013; Stephan et al., 2002). The results of current study identify these cortical regions as parts of the default mode and somatomotor resting-state networks that, within the high period correction network, display strong connectivity with subcortical networks comprising the cerebellum, basal ganglia, and thalamus. Low period correction, on the other hand, leads to weak adaptation to tempo changes presumably due to insufficient internal focus on the process of deliberately adjusting the endogenous timekeeper. Our results indicate that the network profile associated with low period correction is characterized by increased connectivity among default mode regions that overlap with the high period correction network, as well as heightened connectivity between control and salience/ventral attention regions.

The distinction between automatic phase correction and effortful period correction in terms of attentional demands was reflected in the susceptibility of related brain networks to effects of cognitive load. Specifically, the lack of effects of the concurrent visual working memory task on functional connectivity in the high and low phase correction networks suggests that their configuration is robust and proceeds automatically in response to external and internal sources of information. Thus, even though behavioral estimates of phase correction gain increased with attentional demands (perhaps to counter increased timekeeper noise), this increase in gain was not manifest in altered functional connectivity.

By contrast, functional connectivity in period correction networks was modulated by cognitive load. Connectivity increased within and between default and control networks, as well as between control and dorsal attention networks when attentional demands were heightened. Furthermore, while period correction is in theory only required with tempo changes, the brain networks for period correction might still be recruited when coordination challenges arise in the absence of tempo changes, for example, when encountering uncooperative or unreliable synchronization partners (Fairhurst et al., 2014; Repp and Keller, 2008). Accordingly, our finding that the unrestricted analysis of networks in the Virtual Partner task revealed widespread attentional modulation across control, default, dorsal, and ventral attention networks in the absence of modulation of sub-cortical networks suggests that the observed behavioral increase in phase correction gain was underpinned by cortico-subcortical connections associated with period correction.

Taking together results for the high phase correction and high period correction networks, optimal performance may be associated with the ability to alter the balance of focus on external and internal information depending on task goals and momentary demands (Novembre et al., 2016). From a broader perspective, this is consistent with the concepts of metastability (i.e., ability to switch states) and criticality (existing at the boundary between order and disorder) (Deco and Jirsa, 2012;

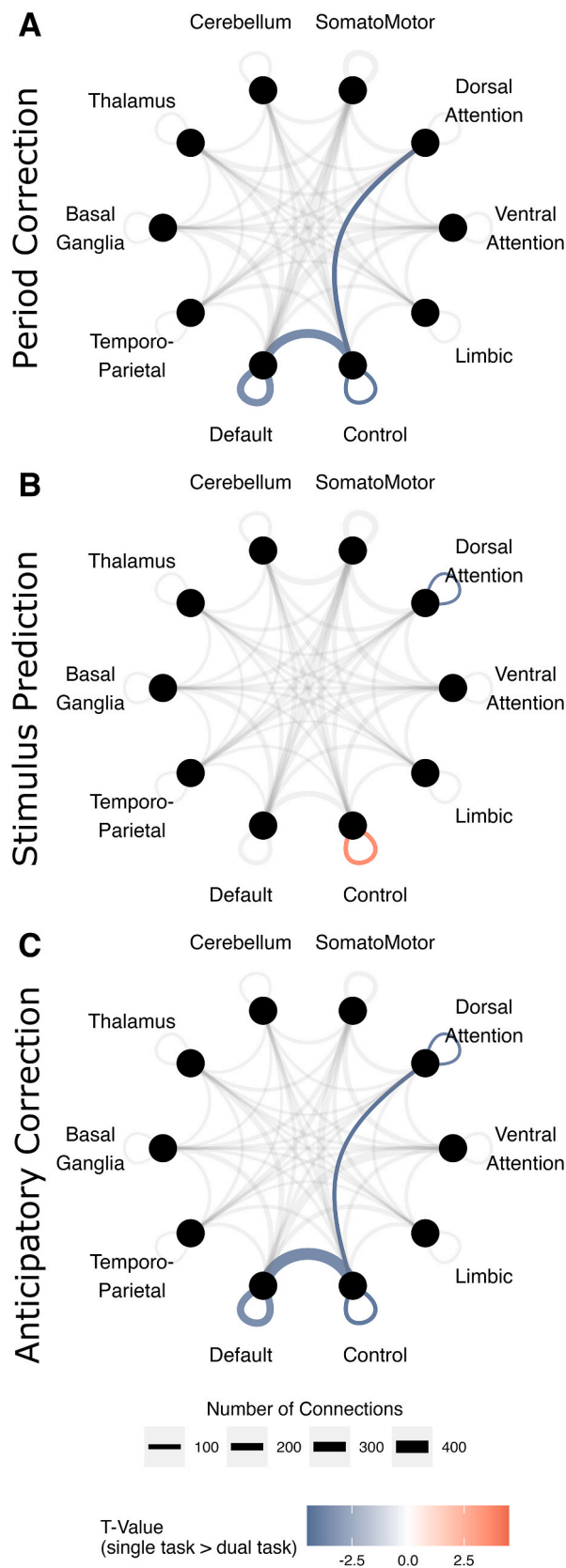


Fig. 11. Attentional modulation of connections (single task > dual task = red, single task < dual task = blue) shown overlaid on the CPM network (grey) identified for **A)** period correction, **B)** stimulus prediction, and **C)** anticipatory error correction for the Tempo Change task.

Tognoli and Kelso, 2014), where the brain is in a state of readiness to respond to changes in the internal and external environment by shifting between endogenous and endogenous focus (Corbetta et al., 2008; Fox et al., 2006; Sridharan et al., 2008).

With regard to temporal prediction, ADAM's anticipation module is primarily externally oriented insofar as it weights the extrapolation versus perseveration of earlier inter-stimulus intervals in environmental event sequences (Harry and Keller, 2019; van der Steen and Keller, 2013). Endogenous processes nevertheless play a role in temporal prediction to the extent that auditory beat prediction involves internally driven action simulation (Cannon and Patel, 2021; Keller, 2012b; Keller et al., 2014; Patel and Iversen, 2014), especially when the simulation process supports beat maintenance based on the perseverative mimicking of the most recent inter-stimulus interval (Repp et al., 2012). Participants whose temporal predictions were relatively high on extrapolation (high stimulus prediction) showed a large proportion of hubs in the control resting-state network and strong connectivity between the control network and somatomotor, cerebellar, and other networks. Participants who demonstrated greater perseverative tracking of tempo changes (low stimulus prediction) had strong connectivity between somatomotor, default mode, ventral attention, and cerebellar networks, in addition to strong connectivity within somatomotor, cerebellar, basal ganglia, and thalamic subcortical networks. Our results thus identify distinct network profiles for the extrapolation and perseveration processes that underpin temporal prediction.

The operation of these dual prediction profiles was apparently immune to effects of cognitive load. Although synchronization with tempo changes is an effortful process that requires working memory (Colley et al., 2018; Pecenka et al., 2013), estimates of stimulus prediction were not affected by the dual task manipulation in the current study. This immunity implies that participants were mainly tracking even in the low cognitive load condition (cf. Mills et al., 2019) or that temporal predictions are not themselves effortful (Marmelat and Delignières, 2012; Roman et al., 2019; Stepp and Turvey, 2010). However, given previous evidence that predictive behavior is reduced and tracking increases under cognitive load (Pecenka et al., 2013), it might be the case that the process of using these predictions to guide action is effortful.

4.2. Simultaneous integration and segregation in the joint network

While brain network reconfiguration related to ADAM's adaptation and anticipation modules is assumed to influence the relative focus on internal and external information, network characteristics associated with the joint module influence the degree of simultaneous integration and segregation of these different information sources. Studies of large-scale brain connectivity have shown that balancing local segregation and global integration in the functional organization of resting-state networks regulates information flow in a manner conducive to flexible task-related behavior (Cohen & D'Esposito, 2016; Deco et al., 2015; Di Plinio, Perrucci, Aleman and Ebisch, 2020; Sporns, 2013; Wang et al., 2021). During sensorimotor synchronization, integration of information about the relationship between one's own action timing and the external sequence is necessary to monitor and evaluate overall performance, whereas segregation is required to maintain autonomous movement control and a distinction between action planning and predictions about external event timing (Heggli et al., 2021; Keller et al., 2016; Liebermann-Jordanidis et al., 2021).

Participants displaying high anticipatory error correction estimates, indicating that a greater proportion of the expected discrepancy between own planned movement timing and predicted event timing was taken into account, had increased connectivity within default mode regions, and between default mode, control, salience/ventral attention, and somatomotor regions. By contrast, participants demonstrating less anticipatory error correction (i.e., only weakly accounting for the anticipated discrepancy between plans and predictions) showed connections primarily between ventral attention, control, somatomotor,

Table 2

Attentional modulation of connections (single task > dual task) identified across all networks (phase correction, period correction, and timekeeper noise combined) identified by CPM in the Virtual Partner task by resting-state interactions.

| Networks | | T-value |
|-------------------|-------------------|---------|
| Control | Dorsal Attention | -3.823 |
| Control | SomatoMotor | -4.053 |
| Control | Control | -3.146 |
| Control | Ventral Attention | -3.285 |
| Default | Dorsal Attention | -3.411 |
| Default | Ventral Attention | -4.565 |
| Default | Default | 3.075 |
| Default | SomatoMotor | -2.850 |
| Dorsal Attention | Dorsal Attention | -2.725 |
| Dorsal Attention | SomatoMotor | -3.359 |
| Dorsal Attention | Temporo-Parietal | -3.579 |
| Limbic | Ventral Attention | -2.965 |
| Ventral Attention | Temporo-Parietal | -3.358 |

and cerebellar regions, and fewer connections with default mode regions.

The overall connectivity pattern observed across high and low anticipatory error correction networks is thus opposite to what was for phase correction and stimulus prediction networks but resembles the pattern observed for period correction (especially in the high period correction network) (Fig. 12). These results suggest a distinction between ADAM brain networks that instantiate effortful processes (period correction and anticipatory error correction) versus more automatic processes (phase correction and stimulus prediction). Consistent with this interpretation, ADAM parameter estimates of anticipatory error correction and period correction were positively correlated (Fig. S13, though note that CPM partialled out effects of different parameters in the model), and functional connectivity within and between networks associated with both processes was modulated similarly by cognitive load. Specifically, as was the case with period correction, the dual task manipulation modulated connectivity in control, dorsal attention, and default mode resting-state networks in the case of anticipatory error correction.

| ADAM Network | | | Resting-State Network | | | |
|---------------------------------|---------------|------|-----------------------|--------|--------|---------|
| | | | DMN | CON | DAN | VAN/SAL |
| | | | Total Number of Edges | | | |
| | | | 16,181 | 14,091 | 10,331 | 12,039 |
| Phase Correction | # Edges | High | 47 | 87 | 142 | 400 |
| | | Low | 252 | 109 | 69 | 45 |
| | % Total Edges | High | 0.29 | 0.62 | 1.37 | 3.32 |
| | | Low | 1.56 | 0.77 | 0.67 | 0.37 |
| Period Correction | # Edges | High | 753 | 235 | 69 | 114 |
| | | Low | 81 | 85 | 36 | 60 |
| | % Total Edges | High | 4.65 | 1.67 | 0.67 | 0.95 |
| | | Low | 0.50 | 0.60 | 0.35 | 0.50 |
| Stimulus Prediction | # Edges | High | 14 | 123 | 0 | 25 |
| | | Low | 320 | 142 | 114 | 263 |
| | % Total Edges | High | 0.09 | 0.87 | 0.00 | 0.21 |
| | | Low | 1.98 | 1.01 | 1.10 | 2.18 |
| Joint (Anticipatory Correction) | # Edges | High | 1260 | 330 | 0 | 34 |
| | | Low | 42 | 98 | 70 | 121 |
| | % Total Edges | High | 7.79 | 2.34 | 0.00 | 0.28 |
| | | Low | 0.26 | 0.70 | 0.68 | 1.01 |

We assume that regions within the ADAM 'rich club' (Table 1 & Fig. 10) enable the joint network to tune the relative integration versus segregation of internal self-related information and external other-related information through interactions with ADAM's adaptation and anticipation modules. This assumption is based on the fact that each of the main resting-state networks is represented by at least one common node in this 'rich club', which provides an exhaustive set of potential links for controlling information flow and network reconfiguration.

Among these node regions, the posterior cingulate cortex/precuneus, the inferior frontal gyrus, the insula, and the temporoparietal junction (spanning parts of the supramarginal gyrus, the lateral occipital cortex, and the angular gyrus) have been previously linked to regulating the integration and segregation of internal and external information in rhythmic contexts (Fairhurst et al., 2013, 2014; Heggli et al., 2021; Hove et al., 2016). A growing body of research on the roles of these regions in large-scale brain network interaction is consistent with this proposed regulatory function. These include the general role of the inferior frontal gyrus in the functional integration of perception and action (Rampinini et al., 2017; Rauschecker and Scott, 2009; Tops and Boksem, 2011) and its interactions with other node regions that tune the brain's level of metastability and trigger switches between task-dependent configurations of resting-state networks. Notably, the posterior cingulate cortex, which sits at the nexus of multiple intrinsic functional connectivity networks (Hagmann et al., 2008; Leech et al., 2011; Margulies et al., 2009), plays a key regulatory role by enabling rapid transitions to neural states that differ in terms of the breadth of attention and the degree to which it is targeted internally or externally (Buckner et al., 2008; Gusnard and Raichle, 2001; Leech and Sharp, 2014).

To facilitate goal-directed processing, the adjoining precuneus interacts with the posterior cingulate to trigger switches between default mode subnetworks that deal with introspective action planning via simulation and extrospective readiness to respond to potential changes in the internal and external environment (Fransson, 2005). In a more stimulus-driven manner, the temporoparietal junction initiates switches in perspective taking when new task-relevant information is detected (Blanke et al., 2005; Corbetta and Shulman, 2002; Tso et al., 2018). The

Fig. 12. General brain networks of interest. A coarse-grained summary representation of how each main resting-state network is recruited in the service of different ADAM modules. The relative number of total connections (edges), expressed as both the actual count (# Edges) and a percentage (% Total Edges), formed by hubs within each ADAM network and each resting-state network is indicated by the level of shading. For # Edges, shaded in greyscale, light shading indicates a low number and dark shading indicates a high number, with values normalized—i.e., scaled separately—for each ADAM network and its high and low subnetworks. For % Total Edges, shaded in color, light shading indicates a low % and dark shading indicates a high %, with values scaled as a proportion of total connections, using the same value across all networks. Note that each ADAM network, and its high and low subnetworks, is associated with a unique pattern of connectivity across resting-state networks. Connectivity increased with increasing values for the relevant ADAM parameter estimates in high networks and connectivity increased with decreasing parameter estimates in low networks. DMN, default mode network; CON, control network; DAN, dorsal attention network; SAL/VAN, salience & ventral attention networks.

insula moderates such interactions through its role in maintaining bodily homeostasis in the face of varying relations between external sensory input and internal physiological signals (Craig, 2009; Singer et al., 2009; Uddin et al., 2017). It does so by influencing how the salience network controls the switching between default mode and control networks (Seeley, 2019; Uddin, 2015), as well by transmitting signals to the posterior cingulate to reduce whole-brain metastability when the need for external attentional focus arises (Uddin et al., 2017). Previous work has charted these interactions in diverse domains ranging from visual perception to social cognition (e.g., Cohen & D'Esposito, 2016; Li et al., 2014; Mori and Haruno, 2022; Sporns, 2013; Van Overwalle, 2009). Current findings highlight how such interactions play out to support real-time rhythmic coordination.

The contributions of subcortical structures to whole-brain network interactions have been less extensively studied. Subcortical members of the ADAM 'rich club' include the crus II subregion of cerebellum, the putamen in the basal ganglia, and the medial pulvinar division of the thalamus. The cerebellum is generally well-equipped for the proposed regulatory role due to its heterogeneous input-output connectivity, which enables segregation via multiple processing streams, together with its homogenous neural circuitry, which enables integration through processing by a common computational substrate (Ito, 1984; Molinari et al., 2007; Tanaka et al., 2020; Van Overwalle et al., 2020). Crus II contributes to such processing particularly in the context of self-other discrimination, mentalizing, and the fine-tuning sequences of social actions and interactions (Peterburs and Desmond, 2016; Van Overwalle et al., 2020). The putamen, which displays high functional connectivity both with regions within the ADAM 'rich club' and ADAM modules (see Cacciola et al., 2017), plays a specific role in facilitating action selection and patterning by optimizing movement sequencing and timing based on information received from the cerebellum directly and indirectly via the thalamus (Bostan and Strick, 2018; Milardi et al., 2019; Rauschecker, 2011). In the context of sensorimotor synchronization, the role of the putamen in beat maintenance (Cannon and Patel, 2021; Grahn and Rowe, 2013) may be functionally relevant to timing interactions and information flow across ADAM brain networks.

Finally, the thalamus regulates functional connectivity within and between cortical resting-state networks in a manner that allows information processed throughout the cortex to be integrated while the modular structure of functional networks is maintained (Guimerà and Nunes Amaral, 2005; Guimerà et al., 2007; Hwang, Bertolero, Liu, & D'Esposito, 2017; Nakajima and Halassa, 2017). It is well-suited to support collaboration between ADAM modules via a gating process that allows coordinated interactions between elementary sensorimotor processes and higher-level cognitive operations (e.g., attention and working memory), albeit with marked individual differences (de Manzano et al., 2010; Hwang et al., 2017; Nakajima and Halassa, 2017; Sherman, 2016).

4.3. Internal models of self, other, and self-other integration

Using ADAM to link behavioral patterns to functional connectivity profiles of resting-state networks has shed light on the brain bases of individual differences in sensorimotor synchronization skills. These skills are crucial for human activities involving rhythmic interpersonal coordination, including musical ensemble performance and group dance. Going beyond present findings, we propose a neurophysiological model that provides a tool for understanding task-based configurations of resting-state networks associated with ADAM's adaptation, anticipation, and joint modules, as well as for scaling up from basic sensory-motor mechanisms to processes that support multi-person interaction in such social contexts (Keller et al., 2014; Müller et al., 2021; Pesquita et al., 2018; Sängner et al., 2011). A caveat related to our hypothetical scheme is that the present study involved synchronization with computer-controlled auditory sequences rather than real human partners. Our investigation is therefore limited in terms of naturalness of the

interaction (D'Ausilio et al., 2015) and richness of sensory experiences, which are often multisensory and involve visual and haptic contact in addition to shared auditory information (Clayton et al., 2020).

In our scheme, the regulatory functions performed by ADAM 'rich club' hub regions are fulfilled by internal models instantiated in cerebro-cerebellar networks that facilitate planning and prediction in skilled action and social interaction by simulating transformations between motor processes and sensory experiences in partial independence of ongoing perception and action (Gambi and Pickering, 2011; Ito, 2008; Keller, 2008; Peterburs and Desmond, 2016; Popa and Ebner, 2019; Tanaka et al., 2020; Wolpert et al., 2003). Specifically, cortical loops that simulate contingencies between body movements and sounds in accordance with ADAM's processing routines are linked to cerebellar internal models that continuously monitor and copy the dynamics of cerebral cortical activity, generating predictions about future sensorimotor and social-cognitive states that are returned to the cortex in compressed form (Ito, 2008; Pollok et al., 2005; Tanaka et al., 2020). These compressed predictions are compared with goal states and actual states, with discrepancies resulting in error signals that return to the cerebellum to allow rapid anticipatory adjustments, to modify subsequent predictions, and to allocate attention as required (Kotz et al., 2014; Peterburs and Desmond, 2016; Van Overwalle et al., 2020).

ADAM's adaptation module informs a 'self' internal model (Fig. 1A) that plans the timing of one's own next action by implementing inverse models, which transform action timing goals into motor programs, and forward models, which represent causal relationships between motor commands and their sensory effects, in the cerebellum and a cortical circuit that includes the premotor cortex, inferior frontal gyrus, and supplementary motor area (Ito, 2008; Todd and Lee, 2015a). In this system, timing goals are updated based on the comparison of feedback from superior temporal auditory regions and somatosensory cortex with desired states in the inferior frontal gyrus, whereas motor programs are updated based on the comparison of predictions generated by 'self' forward models with desired states. These comparisons take place sub-cortically in the basal ganglia (Milardi et al., 2019) and cortically in superior temporal and inferior parietal regions (Rauschecker and Scott, 2009). Our results suggest that phase correction might thus rely to a greater degree on cerebellar internal models to enable rapid, automatic processing, while period correction recruits cortical circuits that are flexible but relatively effortful to implement.

In our account, ADAM's anticipation module informs internal models of others' actions (Table 1A) within cerebro-cerebellar loops that allow an individual to predict the actions of interaction partners via feedforward processes (Ito, 2008; Van Overwalle et al., 2020). Within the cortical circuits, predictions about the timing of others' upcoming actions can evolve via two routes. A goal-directed, top-down form of action simulation calls on the action observation network and the putative mirror neuron system, in tandem with prefrontal working memory regions and intention- or attention-related modulations of activity in the temporoparietal junction and the posterior superior temporal sulcus (Cross et al., 2009; Grèzes et al., 2003; Ito, 2008; Sakai et al., 2002; Schubotz, 2007). In parallel, an automatic bottom-up process of motor resonance (Cannon and Patel, 2021; Patel and Iversen, 2014; Phillips-Silver and Keller, 2012; Todd and Lee, 2015a) instead bases predictions on incoming perceptual information that is used to estimate others' current states in posterior superior temporal regions (Price, 2012; Van Overwalle et al., 2020).

During sensorimotor synchronization, the top-down route thus enables temporal extrapolation to accommodate tempo-changing intervals, while the bottom-up route supports perseveration based on the preceding interval (van der Steen and Keller, 2013). In addition to these cortical contributions, the immunity of ADAM's anticipation module to effects of cognitive load might reflect reliance on rapid temporal predictions enabled by subcortical processes including cerebellar internal models (Ito, 2008; Schubotz, 2007) and a thalamostriatal beat processing loop (Cannon and Patel, 2021; Patel and Iversen, 2014).

Joint internal models implemented by ADAM's joint module (Table 1A) allow potential asynchronies to be simulated and corrected before they occur (Keller et al., 2016; van der Steen and Keller, 2013). This process entails first integrating the outputs of 'self' and 'other' internal models, and then modifying 'own' inverse models to compensate for any discrepancies between these outputs. In terms of neurophysiological implementation, the posterior cingulate cortex, precuneus, and superior frontal gyrus might work together to evaluate own and other predicted states against a representation of a joint desired state (e.g., low asynchrony), with the superior frontal gyrus signalling the magnitude of the anticipated error (Fairhurst et al., 2013; Van Overwalle, 2009) while the posterior cingulate cortex and precuneus regulate the balance between internal models of self and other (Fairhurst et al., 2013; Heggli et al., 2021). In fulfilling its functions in signalling the need for network switches and changes in brain metastability, the insula might evaluate self, other, and joint state estimates based on actual sensory feedback via a closed-loop process that requires externally focused attention (Menon and Uddin, 2010). Together, these feedforward and feedback loops optimize performance by adjusting the gain of own plans and other predictions by altering the connectivity within and between relevant cortical and cerebro-cerebellar circuits based on confidence, or probability estimates, that vary with task context (e.g., the systematicity of tempo changes) and cognitive load (Tanaka et al., 2020; Van Overwalle et al., 2020).

4.4. Conclusions

The current fMRI study used connectome-based predictive modelling to examine patterns of brain functional connectivity related to individual differences in behavioral performance and parameter estimates derived from the adaptation and anticipation model (ADAM) of sensorimotor synchronization. This approach allowed us to identify distinct but overlapping brain networks that support temporal error correction, prediction, and the monitoring and integration of information about one's own action and external events during rhythmic coordination with auditory sequences. Our results suggest that ADAM's adaptation, anticipation, and joint modules house common hub regions that modulate functional connectivity within and between resting-state networks and additional sensory-motor regions and subcortical structures in a manner that reflects coordination skill. At a general level, these connectivity modulations facilitate the temporal alignment of self (own actions) and other (external events) by enabling shifts in the degree of focus on internal and external information, and variations in the degree of simultaneous integration and segregation of these different information sources. Our study was limited to interaction with computer-controlled stimuli, and it therefore remains an open question whether the observed patterns of network reconfiguration generalize to social interaction with real human partners. To the extent that they do, such reconfiguration might support precise yet flexible real-time interpersonal coordination by optimizing the operation of internal models for planning one's own actions, predicting others' action timing, and minimizing the discrepancy between these plans and predictions under conditions that vary in temporal regularity and concurrent cognitive demands.

Credit author statement

Bronson B. Harry: Conceptualization, Methodology, Investigation, Formal analysis, Data curation, Writing – original draft, Visualization, Project administration. **Daniel S. Margulies:** Conceptualization, Methodology, Writing – review & editing. **Marcel Falkiewicz:** Conceptualization, Methodology. **Peter E. Keller:** Conceptualization, Methodology, Formal analysis, Writing – original draft, Writing – review & editing, Supervision, Project administration, Funding acquisition.

Human ethics statement

The study was approved by the Human Research Ethics Committee at Western Sydney University (protocol number H10487), and all participants provided informed written consent.

Data availability

Data will be made available on request.

Acknowledgements

This research was supported by a Future Fellowship grant from the Australian Research Council (FT140101162) awarded to P.E.K. The Center for Music in the Brain is funded by the Danish National Research Foundation (DNRF117). The authors thank Peta Mills and Jennifer Lee for assistance with data collection.

Appendix A. Supplementary data

Supplementary data to this article can be found online at <https://doi.org/10.1016/j.neuropsychologia.2023.108524>.

References

- Alluri, V., Toivainen, P., Jaaskelainen, I.P., Glerean, E., Sams, M., Brattico, E., 2012. Large-scale brain networks emerge from dynamic processing of musical timbre, key and rhythm. *Neuroimage* 59, 3677–3689. <https://doi.org/10.1016/j.neuroimage.2011.11.019>.
- Bassett, D.S., Sporns, O., 2017. Network neuroscience. *Nat. Neurosci.* 20 (3), 353–364. <https://doi.org/10.1038/nn.4502>.
- Behrens, T.E., Johansen-Berg, H., Woolrich, M.W., Smith, S.M., Wheeler-Kingshott, C.A.M., Boulby, P.A., Matthews, P.M., 2003a. Non-invasive mapping of connections between human thalamus and cortex using diffusion imaging. *Nat. Neurosci.* 6 (7), 750–757. <https://doi.org/10.1038/nn1075>.
- Behrens, T.E., Woolrich, M.W., Jenkinson, M., Johansen-Berg, H., Nunes, R.G., Clare, S., Smith, S.M., 2003b. Characterization and propagation of uncertainty in diffusion-weighted MR imaging. *Magn. Reson. Med.* 50 (5), 1077–1088. <https://doi.org/10.1002/mrm.10609>.
- Bertolero, M.A., Yeo, B.T.T., Desposito, M., 2017. The diverse club. *Nat. Commun.* 8 (1), 1277. <https://doi.org/10.1038/s41467-017-01189-w>.
- Bijsterbosch, J.D., Lee, K.-H., Hunter, M.D., Tsoi, D.T., Lankappa, S., Wilkinson, I.D., Woodruff, P.W.R., 2011. The role of the cerebellum in sub- and supraliminal error correction during sensorimotor synchronization: evidence from fMRI and TMS. *J. Cognit. Neurosci.* 23, 1100–1112. <https://doi.org/10.1162/jocn.2010.21506>.
- Blanke, O., Mohr, C., Michel, C.M., Pascual-Leone, A., Brugger, P., Seeck, M., Thut, G., 2005. Linking out-of-body experience and self processing to mental own-body imagery at the temporoparietal junction. *J. Neurosci.* 25 (3), 550–557. <https://doi.org/10.1523/jneurosci.2612-04.2005>.
- Bostan, A.C., Strick, P.L., 2018. The basal ganglia and the cerebellum: nodes in an integrated network. *Nat. Rev. Neurosci.* 19 (6), 338–350. <https://doi.org/10.1038/s41583-018-0002-7>.
- Buckner, R.L., Andrews-Hanna, J.R., Schacter, D.L., 2008. The brain's default network: anatomy, function, and relevance to disease. *Ann. N. Y. Acad. Sci.* 1124, 1–38. <https://doi.org/10.1196/annals.1440.011>.
- Cacciola, A., Calamuneri, A., Milardi, D., Mormina, E., Chillemi, G., Marino, S., Quartarone, A., 2017. A connectomic analysis of the human basal ganglia network. *Front. Neuroanat.* 11 <https://doi.org/10.3389/fnana.2017.00085>, 85–85.
- Cannon, J.J., Patel, A.D., 2021. How beat perception co-opts motor neurophysiology. *Trends Cognit. Sci.* 25 (2), 137–150. <https://doi.org/10.1016/j.tics.2020.11.002>.
- Chauvigne, L.A., Gitau, K.M., Brown, S., 2014. The neural basis of audiomotor entrainment: an ALE meta-analysis. *Front. Hum. Neurosci.* 8, 776. <https://doi.org/10.3389/fnhum.2014.00776>.
- Chen, J.L., Penhune, V.B., Zatorre, R.J., 2008. Moving on time: brain network for auditory-motor synchronization is modulated by rhythm complexity and musical training. *J. Cognit. Neurosci.* 20, 226–239. <https://doi.org/10.1162/jocn.2008.20018>.
- Clayton, M., Jakubowski, K., Eerola, T., Keller, P.E., Camurri, A., Volpe, G., Alborn, P., 2020. Interpersonal entrainment in music performance. *Music Perception* 38 (2), 136–194. <https://doi.org/10.1525/mp.2020.38.2.136>.
- Cohen, J.R., Desposito, M., 2016. The segregation and integration of distinct brain networks and their relationship to cognition. *J. Neurosci.* 36 (48), 12083–12094. <https://doi.org/10.1523/jneurosci.2965-15.2016>.
- Cole, M.W., Bassett, D.S., Power, J.D., Braver, T.S., Petersen, S.E., 2014. Intrinsic and task-evoked network architectures of the human brain. *Neuron* 83 (1), 238–251. <https://doi.org/10.1016/j.neuron.2014.05.014>.

- Colley, I.D., Keller, P.E., Halpern, A.R., 2018. Working memory and auditory imagery predict sensorimotor synchronisation with expressively timed music. *Q. J. Exp. Psychol.* 71 (8), 1781–1796. <https://doi.org/10.1080/17470218.2017.1366531>.
- Comstock, D.C., Hove, M.J., Balasubramanian, R., 2018. Sensorimotor synchronization with auditory and visual modalities: behavioral and neural differences. *Front. Comput. Neurosci.* 12 (53) <https://doi.org/10.3389/fncom.2018.00053>.
- Corbetta, M., Patel, G., Shulman, G.L., 2008. The reorienting system of the human brain: from environment to theory of mind. *Neuron* 58 (3), 306–324. <https://doi.org/10.1016/j.neuron.2008.04.017>.
- Corbetta, M., Shulman, G.L., 2002. Control of goal-directed and stimulus-driven attention in the brain. *Nat. Rev. Neurosci.* 3 (3), 201–215. <https://doi.org/10.1038/nrn755>.
- Coull, J.T., 2004. fMRI studies of temporal attention: allocating attention within, or towards, time. *Brain Research. Cognitive Brain Research* 21, 216–226. <https://doi.org/10.1016/j.cogbrainres.2004.02.011>.
- Coull, J.T., Cheng, R.-K., Meck, W.H., 2011. Neuroanatomical and neurochemical substrates of timing. *Neuropsychopharmacology* 36, 3–25. <https://doi.org/10.1038/npp.2010.113>.
- Craig, A.D., 2009. How do you feel—now? The anterior insula and human awareness. *Nat. Rev. Neurosci.* 10 (1), 59–70. <https://doi.org/10.1038/nrn2555>.
- Cross, E.S., Kraemer, D.J., Hamilton, A.F., Kelley, W.M., Grafton, S.T., 2009. Sensitivity of the action observation network to physical and observational learning. *Cerebr. Cortex* 19, 315–326. <https://doi.org/10.1093/cercor/bhn083>.
- Crossley, N.A., Mechelli, A., Vertes, P.E., Winton-Brown, T.T., Patel, A.X., Gineestet, C.E., Bullmore, E.T., 2013. Cognitive relevance of the community structure of the human brain functional coactivation network. *Proc. Natl. Acad. Sci. U.S.A.* 110 (28), 11583–11588. <https://doi.org/10.1073/pnas.1220826110>.
- Dausilio, A., Novembre, G., Fadiga, L., Keller, P.E., 2015. What can music tell us about social interaction? *Trends Cognit. Sci.* 19 (3), 111–114.
- de Manzano, O., Cervenka, S., Karabanov, A., Farde, L., Ullen, F., 2010. Thinking outside a less intact box: thalamic dopamine D2 receptor densities are negatively related to psychometric creativity in healthy individuals. *PLoS One* 5 (5), e10670. <https://doi.org/10.1371/journal.pone.0010670>.
- Deco, G., Jirsa, V.K., 2012. Ongoing cortical activity at rest: criticality, multistability, and ghost attractors. *J. Neurosci.* 32 (10), 3366–3375. <https://doi.org/10.1523/jneurosci.2523-11.2012>.
- Deco, G., Tononi, G., Boly, M., Kringelbach, M.L., 2015. Rethinking segregation and integration: contributions of whole-brain modelling. *Nat. Rev. Neurosci.* 16 (7), 430–439. <https://doi.org/10.1038/nrn3963>.
- Di Plinio, S., Perrucci, M.G., Aleman, A., Ebisch, S.J.H., 2020. I am Me: brain systems integrate and segregate to establish a multidimensional sense of self. *Neuroimage* 205, 116284. <https://doi.org/10.1016/j.neuroimage.2019.116284>.
- Diedrichsen, J., Balsters, J.H., Flavell, J., Cussans, E., Ramnani, N., 2009. A probabilistic MR atlas of the human cerebellum. *Neuroimage* 46 (1), 39–46. <https://doi.org/10.1016/j.neuroimage.2009.01.045>.
- Dixon, M.L., Andrews-Hanna, J.R., Spreng, R.N., Irving, Z.C., Mills, C., Girm, M., Christoff, K., 2017. Interactions between the default network and dorsal attention network vary across default subsystems, time, and cognitive states. *Neuroimage* 147, 632–649. <https://doi.org/10.1016/j.neuroimage.2016.12.073>.
- Dumas, G., de Guzman, G.C., Tognoli, E., Kelso, J.A., 2014. The human dynamic clamp as a paradigm for social interaction. *Proc. Natl. Acad. Sci. U.S.A.* 111 (35), E3726–E3734. <https://doi.org/10.1073/pnas.1407486111>.
- Dumas, G., Moreau, Q., Tognoli, E., Kelso, J.A.S., 2019. The human dynamic clamp reveals the fronto-parietal network linking real-time social coordination and cognition. *Cerebr. Cortex*. <https://doi.org/10.1093/cercor/bhz308>.
- Fairhurst, M.T., Janata, P., Keller, P.E., 2013. Being and feeling in sync with an adaptive virtual partner: brain mechanisms underlying dynamic cooperativity. *Cerebr. Cortex* 23, 2592–2600. <https://doi.org/10.1093/cercor/bhs243>.
- Fairhurst, M.T., Janata, P., Keller, P.E., 2014. Leading the follower: an fMRI investigation of dynamic cooperativity and leader-follower strategies in synchronization with an adaptive virtual partner. *Neuroimage* 84, 688–697. <https://doi.org/10.1016/j.neuroimage.2013.09.027>.
- Finm, E.S., Shen, X., Scheinost, D., Rosenberg, M.D., Huang, J., Chun, M.M., Constable, R. T., 2015. Functional connectome fingerprinting: identifying individuals using patterns of brain connectivity. *Nat. Neurosci.* 18 (11), 1664–1671. <https://doi.org/10.1038/nn.4135>.
- Fornito, A., Harrison, B.J., Zalesky, A., Simons, J.S., 2012. Competitive and cooperative dynamics of large-scale brain functional networks supporting recollection. *Proc. Natl. Acad. Sci. U.S.A.* 109 (31), 12788–12793. <https://doi.org/10.1073/pnas.1204185109>.
- Fox, M.D., Corbetta, M., Snyder, A.Z., Vincent, J.L., Raichle, M.E., 2006. Spontaneous neuronal activity distinguishes human dorsal and ventral attention systems. *Proc. Natl. Acad. Sci. U.S.A.* 103 (26), 10046–10051. <https://doi.org/10.1073/pnas.0604187103>.
- Fransson, P., 2005. Spontaneous low-frequency BOLD signal fluctuations: an fMRI investigation of the resting-state default mode of brain function hypothesis. *Hum. Brain Mapp.* 26 (1), 15–29. <https://doi.org/10.1002/hbm.20113>.
- Gallotti, M., Fairhurst, M.T., Frith, C.D., 2016. Alignment in social interactions. *Conscious. Cognit.* 48, 253–261. <https://doi.org/10.1016/j.concog.2016.12.002>.
- Gambi, C., Pickering, M.J., 2011. A cognitive architecture for the coordination of utterances. *Front. Psychol.* 2, 275. <https://doi.org/10.3389/fpsyg.2011.00275>.
- Grahn, J.A., Brett, M., 2007. Rhythm and beat perception in motor areas of the brain. *J. Cognit. Neurosci.* 19, 893–906.
- Grahn, J.A., Rowe, J.B., 2013. Finding and feeling the musical beat: striatal dissociations between detection and prediction of regularity. *Cerebr. Cortex* 23, 913–921. <https://doi.org/10.1093/cercor/bhs083>.
- Grezes, J., Tucker, M., Armony, J., Ellis, R., Passingham, R.E., 2003. Objects automatically potentiate action: an fMRI study of implicit processing. *Eur. J. Neurosci.* 17 (12), 2735–2740. <https://doi.org/10.1046/j.1460-9568.2003.02695.x>.
- Guimera, R., Nunes Amaral, L.A., 2005. Functional cartography of complex metabolic networks. *Nature* 433 (7028), 895–900. <https://doi.org/10.1038/nature03288>.
- Guimera, R., Sales-Pardo, M., Amaral, L.A.N., 2007. Classes of complex networks defined by role-to-role connectivity profiles. *Nat. Phys.* 3 (1), 63–69. <https://doi.org/10.1038/nphys489>.
- Gusnard, D.A., Raichle, M.E., 2001. Searching for a baseline: functional imaging and the resting human brain. *Nat. Rev. Neurosci.* 2 (10), 685–694. <https://doi.org/10.1038/35094500>.
- Hagmann, P., Cammoun, L., Gigandet, X., Meuli, R., Honey, C.J., Wedeen, V.J., Sporns, O., 2008. Mapping the structural core of human cerebral cortex. *PLoS Biol.* 6 (7), e159. <https://doi.org/10.1371/journal.pbio.0060159>.
- Harry, B., Keller, P.E., 2019. Tutorial and simulations with ADAM: an adaptation and anticipation model of sensorimotor synchronization. *Biol. Cybern.* 113 (4), 397–421. <https://doi.org/10.1007/s00422-019-00798-6>.
- Heggli, O.A., Cabral, J., Konvalinka, I., Vuust, P., Kringelbach, M.L., 2019. A Kuramoto model of self-other integration across interpersonal synchronization strategies. *PLoS Comput. Biol.* 15 (10), e1007422. <https://doi.org/10.1371/journal.pcbi.1007422>.
- Heggli, O.A., Konvalinka, I., Cabral, J., Brattico, E., Kringelbach, M.L., Vuust, P., 2020. Transient brain networks underlying interpersonal strategies during synchronized action. *Soc. Cognit. Affect Neurosci.* 16 (1–2), 19–30. <https://doi.org/10.1093/scan/nsaa056>.
- Heggli, O.A., Konvalinka, I., Kringelbach, M.L., Vuust, P., 2021. A metastable attractor model of self-other integration (MEAMSO) in rhythmic synchronization. *Philos. Trans. R. Soc. Lond. Ser. B Biol. Sci.* 376 (1835), 20200332. <https://doi.org/10.1098/rstb.2020.0332>.
- Hill, K.T., Miller, L.M., 2010. Auditory attentional control and selection during cocktail party listening. *Cerebr. Cortex* 20, 583–590. <https://doi.org/10.1093/cercor/bhp124>.
- Hove, M.J., Stelzer, J., Nierhaus, T., Thiel, S.D., Gundlach, C., Margulies, D.S., Merker, B., 2016. Brain network reconfiguration and perceptual decoupling during an absorptive state of consciousness. *Cerebr. Cortex* 26 (7), 3116–3124. <https://doi.org/10.1093/cercor/bhv137>.
- Hwang, K., Bertolero, M.A., Liu, W.B., Desposito, M., 2017. The human thalamus is an integrative hub for functional brain networks. *J. Neurosci.* 37 (23), 5594–5607. <https://doi.org/10.1523/JNEUROSCI.0067-17.2017>.
- Ito, M., 1984. *The Cerebellum and Neural Control*. Raven Press, New York.
- Ito, M., 2008. Control of mental activities by internal models in the cerebellum. *Nature reviews Neuroscience* 9, 304–313. <https://doi.org/10.1038/nrn2332>.
- Jacoby, N., Repp, B.H., 2012. A general linear framework for the comparison and evaluation of models of sensorimotor synchronization. *Biol. Cybern.* 106, 135–154. <https://doi.org/10.1007/s00422-012-0482-x>.
- Jacoby, N., Tishby, N., Repp, B.H., Ahissar, M., Keller, P.E., 2015. Parameter estimation of linear sensorimotor synchronization models: phase correction, period correction, and ensemble synchronization. *Timing & Time Percept.* 3 (1–2), 52–87. <https://doi.org/10.1163/22134468-00002048>.
- Janata, P., Tillmann, B., Bharucha, J.J., 2002. Listening to polyphonic music recruits domain-general attention and working memory circuits. *Cognit. Affect Behav. Neurosci.* 2, 121–140.
- Jancke, L., Loose, R., Lutz, K., Specht, K., Shah, N.J., 2000. Cortical activations during paced finger-tapping applying visual and auditory pacing stimuli. *Cognit. Brain Res.* 10, 51–66.
- Jasmin, K.M., McGettigan, C., Agnew, Z.K., Lavan, N., Josephs, O., Cummins, F., Scott, S. K., 2016. Cohesion and joint speech: right hemisphere contributions to synchronized vocal production. *J. Neurosci.* 36 (17), 4669–4680. <https://doi.org/10.1523/JNEUROSCI.4075-15.2016>.
- Keller, P.E., 2008. Joint action in music performance. In: Morganti, F., Carassa, A., Riva, G. (Eds.), *Enacting Intersubjectivity: A Cognitive and Social Perspective to the Study of Interactions*. IOS Press, Amsterdam, pp. 205–221.
- Keller, P.E., 2012a. Mental imagery in music performance: underlying mechanisms and potential benefits. *Ann. N. Y. Acad. Sci.* 1252, 206–213. <https://doi.org/10.1111/j.1749-6632.2011.06439.x>.
- Keller, P.E., 2012b. Rhythm and time in music epitomize the temporal dynamics of human communicative behavior: the broad implications of London's Trinity. *Empirical Musicology Review* 7, 17–27.
- Keller, P.E., Novembre, G., Hove, M.J., 2014. Rhythm in joint action: psychological and neurophysiological mechanisms for real-time interpersonal coordination. *Philos. Trans. R. Soc. Lond. Ser. B Biol. Sci.* 369 (1658), 20130394. <https://doi.org/10.1098/rstb.2013.0394>.
- Keller, P.E., Novembre, G., Loehr, J., 2016. Musical ensemble performance: representing self, other and joint action outcomes. In: Obhi, S.S., Cross, E.S. (Eds.), *Shared Representations: Sensorimotor Foundations of Social Life*. Cambridge University Press, Cambridge, pp. 280–310.
- Konvalinka, I., Bauer, M., Stahlhut, C., Hansen, L.K., Roepstorff, A., Frith, C.D., 2014. Frontal alpha oscillations distinguish leaders from followers: multivariate decoding of mutually interacting brains. *Neuroimage* 94, 79–88. <https://doi.org/10.1016/j.neuroimage.2014.03.003>.
- Konvalinka, I., Vuust, P., Roepstorff, A., Frith, C.D., 2010. Follow you, follow me: continuous mutual prediction and adaptation in joint tapping. *Q. J. Exp. Psychol.* 63, 2220–2230. <https://doi.org/10.1080/17470218.2010.497843>.
- Kotz, S.A., Stockert, A., Schwartz, M., 2014. Cerebellum, temporal predictability and the updating of a mental model. *Philos. Trans. R. Soc. Lond. Ser. B Biol. Sci.* 369 (1658), 20130403. <https://doi.org/10.1098/rstb.2013.0403>.

- Leech, R., Kamourieh, S., Beckmann, C.F., Sharp, D.J., 2011. Fractionating the default mode network: distinct contributions of the ventral and dorsal posterior cingulate cortex to cognitive control. *J. Neurosci.* 31 (9), 3217–3224. <https://doi.org/10.1523/jneurosci.5626-10.2011>.
- Leech, R., Sharp, D.J., 2014. The role of the posterior cingulate cortex in cognition and disease. *Brain* 137 (Pt 1), 12–32. <https://doi.org/10.1093/brain/awt162>.
- Levitin, D.J., Grahm, J.A., London, J., 2018. The psychology of music: rhythm and movement. *Annu. Rev. Psychol.* 69 (1), 51–75. <https://doi.org/10.1146/annurev-psych-122216-011740>.
- Li, W., Mai, X., Liu, C., 2014. The default mode network and social understanding of others: what do brain connectivity studies tell us. *Front. Hum. Neurosci.* 8, 74. <https://doi.org/10.3389/fnhum.2014.00074>.
- Liebermann-Jordanidis, H., Novembre, G., Koch, I., Keller, P.E., 2021. Simultaneous self-other integration and segregation support real-time interpersonal coordination in a musical joint action task. *Acta Psychol.* 218, 103348. <https://doi.org/10.1016/j.actpsy.2021.103348>.
- Loehr, J.D., Large, E.W., Palmer, C., 2011. Temporal coordination and adaptation to rate change in music performance. *J. Exp. Psychol. Human Perception and Performance* 37, 1292–1309. <https://doi.org/10.1037/a0023102>.
- Margulies, D.S., Vincent, J.L., Kelly, C., Lohmann, G., Uddin, L.Q., Biswal, B.B., Petrides, M., 2009. Precuneus shares intrinsic functional architecture in humans and monkeys. *Proc. Natl. Acad. Sci. USA* 106 (47), 20069–20074. <https://doi.org/10.1073/pnas.0905314106>.
- Marmelat, V., Delignieres, D., 2012. Strong anticipation: complexity matching in interpersonal coordination. *Exp. Brain Res.* 222 (1–2), 137–148. <https://doi.org/10.1007/s00221-012-3202-9>.
- Mates, J., 1994a. A model of synchronization of motor acts to a stimulus sequence: II. Stability analysis, error estimation and simulations. *Biol. Cybern.* 70 (5), 475–484. <https://doi.org/10.1007/bf00203240>.
- Mates, J., 1994b. A model of synchronization of motor acts to a stimulus sequence. I. Timing and error corrections. *Biol. Cybern.* 70, 463–473.
- Matthews, T.E., Witek, M.A.G., Lund, T., Vuust, P., Penhune, V.B., 2020. The sensation of groove engages motor and reward networks. *Neuroimage* 214, 116768. <https://doi.org/10.1016/j.neuroimage.2020.116768>.
- Menon, V., Uddin, L.Q., 2010. Saliency, switching, attention and control: a network model of insula function. *Brain Struct. Funct.* 214 (5–6), 655–667. <https://doi.org/10.1007/s00429-010-0262-0>.
- Milardi, D., Quartarone, A., Bramanti, A., Anastasi, G., Bertino, S., Basile, G.A., Cacciola, A., 2019. The cortico-basal ganglia-cerebellar network: past, present and future perspectives. *Front. Syst. Neurosci.* 13 (61) <https://doi.org/10.3389/fnsys.2019.00061>.
- Mills, P.F., Harry, B., Stevens, C.J., Knoblich, G., Keller, P.E., 2019. Intentionality of a co-actor influences sensorimotor synchronisation with a virtual partner. *Q. J. Exp. Psychol.* 72 (6), 1478–1492. <https://doi.org/10.1177/1747021818796183>.
- Mills, P.F., van der Steen, M.C., Schultz, B.G., Keller, P.E., 2015. Individual differences in temporal anticipation and adaptation during sensorimotor synchronization. *Timing & Time Percept.* 3 (1–2), 13–31. <https://doi.org/10.1163/22134468-03002040>.
- Miyata, K., Yamamoto, T., Fukunaga, M., Sugawara, S., Sadato, N., 2022. Neural correlates with individual differences in temporal prediction during auditory-motor synchronization. *Cerebral Cortex Communications*. <https://doi.org/10.1093/texcom/tgac014>.
- Molinari, M., Leggio, M.G., Thaut, M.H., 2007. The cerebellum and neural networks for rhythmic sensorimotor synchronization in the human brain. *Cerebellum* 6, 18–23. <https://doi.org/10.1080/14734220601142886>.
- Mori, K., Haruno, M., 2022. Resting functional connectivity of the left inferior frontal gyrus with the dorsomedial prefrontal cortex and temporoparietal junction reflects the social network size for active interactions. *Hum. Brain Mapp.* 43 (9), 2869–2879. <https://doi.org/10.1002/hbm.25822>.
- Muller, V., Ohstrome, K.-R.P., Lindenberger, U., 2021. Interactive brains, social minds: neural and physiological mechanisms of interpersonal action coordination. *Neurosci. Biobehav. Rev.* 128, 661–677. <https://doi.org/10.1016/j.neubiorev.2021.07.017>.
- Nakajima, M., Halassa, M.M., 2017. Thalamic control of functional cortical connectivity. *Curr. Opin. Neurobiol.* 44, 127–131. <https://doi.org/10.1016/j.conb.2017.04.001>.
- Novembre, G., Sammler, D., Keller, P.E., 2016. Neural alpha oscillations index the balance between self-other integration and segregation in real-time joint action. *Neuropsychologia* 89, 414–425. <https://doi.org/10.1016/j.neuropsychologia.2016.07.027>.
- Oullier, O., Jantzen, K.J., Steinberg, F.L., Kelso, J.A., 2005. Neural substrates of real and imagined sensorimotor coordination. *Cerebr. Cortex* 15, 975–985. <https://doi.org/10.1093/cercor/bhh198>.
- Patel, A.D., Iversen, J.R., 2014. The evolutionary neuroscience of musical beat perception: the Action Simulation for Auditory Prediction (ASAP) hypothesis. *Front. Syst. Neurosci.* 8, 57. <https://doi.org/10.3389/fnsys.2014.00057>.
- Pecenk, N., Engel, A., Keller, P.E., 2013. Neural correlates of auditory temporal predictions during sensorimotor synchronization. *Front. Hum. Neurosci.* 7, 380. <https://doi.org/10.3389/fnhum.2013.00380>.
- Pecenk, N., Keller, P.E., 2011. The role of temporal prediction abilities in interpersonal sensorimotor synchronization. *Exp. Brain Res.* 211, 505–515. <https://doi.org/10.1007/s00221-011-2616-0>.
- Penhune, V.B., Zatorre, R.J., Evans, A.C., 1998. Cerebellar contributions to motor timing: a PET study of auditory and visual rhythm reproduction. *J. Cognit. Neurosci.* 10 (6), 752–765. <https://doi.org/10.1162/089892998563149>.
- Pesquita, A., Whitwell, R.L., Enns, J.T., 2018. Predictive joint-action model: a hierarchical predictive approach to human cooperation. *Psychonomic Bull. Rev.* 25 (5), 1751–1769. <https://doi.org/10.3758/s13423-017-1393-6>.
- Peterburs, J., Desmond, J.E., 2016. The role of the human cerebellum in performance monitoring. *Curr. Opin. Neurobiol.* 40, 38–44. <https://doi.org/10.1016/j.conb.2016.06.011>.
- Phillips-Silver, J., Keller, P.E., 2012. Searching for roots of entrainment and joint action in early musical interactions. *Front. Hum. Neurosci.* 6, 26. <https://doi.org/10.3389/fnhum.2012.00026>.
- Pollok, B., Gross, J., Muller, K., Aschersleben, G., Schnitzler, A., 2005. The cerebral oscillatory network associated with auditorily paced finger movements. *Neuroimage* 24 (3), 646–655. <https://doi.org/10.1016/j.neuroimage.2004.10.009>.
- Popa, L.S., Ebner, T.J., 2019. Cerebellum, predictions and errors. *Front. Cell. Neurosci.* 12 (524) <https://doi.org/10.3389/fncel.2018.00524>.
- Praamstra, P., Turgeon, M., Hesse, C.W., Wing, A.M., Perryer, L., 2003. Neurophysiological correlates of error correction in sensorimotor-synchronization. *Neuroimage* 20, 1283–1297. [https://doi.org/10.1016/s1053-8119\(03\)00351-3](https://doi.org/10.1016/s1053-8119(03)00351-3).
- Price, C.J., 2012. A review and synthesis of the first 20 years of PET and fMRI studies of heard speech, spoken language and reading. *Neuroimage* 62 (2), 816–847. <https://doi.org/10.1016/j.neuroimage.2012.04.062>.
- Rampinini, A.C., Handjaras, G., Leo, A., Cecchetti, L., Ricciardi, E., Marotta, G., Pietrini, P., 2017. Functional and spatial segregation within the inferior frontal and superior temporal cortices during listening, articulation imagery, and production of vowels. *Sci. Rep.* 7 (1), 17029. <https://doi.org/10.1038/s41598-017-17314-0>.
- Rao, S.M., Harrington, D.L., Haaland, K.Y., Bobholz, J.A., Cox, R.W., Binder, J.R., 1997. Distributed neural systems underlying the timing of movements. *J. Neurosci.* 17, 5528–5535.
- Rauschecker, J.P., 2011. An expanded role for the dorsal auditory pathway in sensorimotor control and integration. *Hear. Res.* 271, 16–25. <https://doi.org/10.1016/j.heares.2010.09.001>.
- Rauschecker, J.P., Scott, S.K., 2009. Maps and streams in the auditory cortex: nonhuman primates illuminate human speech processing. *Nat. Neurosci.* 12, 718–724. <https://doi.org/10.1038/nn.2331>.
- Repp, B.H., 2005. Sensorimotor synchronization: a review of the tapping literature. *Psychonomic Bull. Rev.* 12, 969–992.
- Repp, B.H., Keller, P.E., 2004. Adaptation to tempo changes in sensorimotor synchronization: effects of intention, attention, and awareness. *The Quarterly Journal of Experimental Psychology. A, Human Experimental Psychology* 57, 499–521. <https://doi.org/10.1080/02724980343000369>.
- Repp, B.H., Keller, P.E., 2008. Sensorimotor synchronization with adaptively timed sequences. *Hum. Mov. Sci.* 27, 423–456. <https://doi.org/10.1016/j.humov.2008.02.016>.
- Repp, B.H., Keller, P.E., Jacoby, N., 2012. Quantifying phase correction in sensorimotor synchronization: empirical comparison of three paradigms. *Acta Psychol.* 139, 281–290. <https://doi.org/10.1016/j.actpsy.2011.11.002>.
- Repp, B.H., Su, Y.H., 2013. Sensorimotor synchronization: a review of recent research (2006–2012). *Psychonomic Bull. Rev.* 20, 403–452. <https://doi.org/10.3758/s13423-012-0371-2>.
- Roman, I.R., Washburn, A., Large, E.W., Chafe, C., Fujioka, T., 2019. Delayed feedback embedded in perception-action coordination cycles results in anticipation behavior during synchronized rhythmic action: a dynamical systems approach. *PLoS Comput. Biol.* 15 (10), e1007371. <https://doi.org/10.1371/journal.pcbi.1007371>.
- Rosenberg, M.D., Finn, E.S., Scheinost, D., Constable, R.T., Chun, M.M., 2017. Characterizing attention with predictive network models. *Trends Cognit. Sci.* 21 (4), 290–302. <https://doi.org/10.1016/j.tics.2017.01.011>.
- Rosenberg, M.D., Finn, E.S., Scheinost, D., Papademetris, X., Shen, X., Constable, R.T., Chun, M.M., 2016. A neuromarker of sustained attention from whole-brain functional connectivity. *Nat. Neurosci.* 19 (1), 165–171. <https://doi.org/10.1038/nn.4179>.
- Sakai, K., Rowe, J.B., Passingham, R.E., 2002. Active maintenance in prefrontal area 46 creates distractor-resistant memory. *Nat. Neurosci.* 5 (5), 479–484. <https://doi.org/10.1038/nn846>.
- Sanger, J., Lindenberger, U., Müller, V., 2011. Interactive brains, social minds. *Commun. Integr. Biol.* 4, 655–663. <https://doi.org/10.4161/cib.4.6.17934>.
- Satoh, M., Takeda, K., Nagata, K., Hatazawa, J., Kuzuhara, S., 2001. Activated brain regions in musicians during an ensemble: a PET study. *Cognit. Brain Res.* 12, 101–108.
- Schaefer, A., Kong, R., Gordon, E.M., Laumann, T.O., Zuo, X.N., Holmes, A.J., Yeo, B.T.T., 2018. Local-global parcellation of the human cerebral cortex from intrinsic functional connectivity MRI. *Cerebr. Cortex* 28 (9), 3095–3114. <https://doi.org/10.1093/cercor/bbx179>.
- Schubotz, R.I., 2007. Prediction of external events with our motor system: towards a new framework. *Trends Cognit. Sci.* 11, 211–218. <https://doi.org/10.1016/j.tics.2007.02.006>.
- Schulze, H.-H., Cordes, A., Vorberg, D., 2005. Keeping synchrony while tempo changes: accelerando and ritardando. *Music Perception* 22, 461–477.
- Seeley, W.W., 2019. The salience network: a neural system for perceiving and responding to homeostatic demands. *J. Neurosci.* 39 (50), 9878–9882. <https://doi.org/10.1523/jneurosci.1138-17.2019>.
- Seitzman, B.A., Snyder, A.Z., Leuthardt, E.C., Shimony, J.S., 2019. The state of resting state networks. *Top. Magn. Reson. Imag.* : TMRI 28 (4), 189–196. <https://doi.org/10.1097/RMR.0000000000000214>.
- Shamay-Tsoory, S.G., Saporta, N., Marton-Alper, I.Z., Gvirts, H.Z., 2019. Herding brains: a core neural mechanism for social alignment. *Trends Cognit. Sci.* 23 (3), 174–186. <https://doi.org/10.1016/j.tics.2019.01.002>.
- Shen, X., Finn, E.S., Scheinost, D., Rosenberg, M.D., Chun, M.M., Papademetris, X., Constable, R.T., 2017. Using connectome-based predictive modeling to predict individual behavior from brain connectivity. *Nat. Protoc.* 12 (3), 506–518. <https://doi.org/10.1038/nprot.2016.178>.

- Sherman, S.M., 2016. Thalamus plays a central role in ongoing cortical functioning. *Nat. Neurosci.* 19 (4), 533–541. <https://doi.org/10.1038/nn.4269>.
- Singer, T., Critchley, H.D., Preuschoff, K., 2009. A common role of insula in feelings, empathy and uncertainty. *Trends Cognit. Sci.* 13 (8), 334–340. <https://doi.org/10.1016/j.tics.2009.05.001>.
- Sporns, O., 2013. Network attributes for segregation and integration in the human brain. *Curr. Opin. Neurobiol.* 23 (2), 162–171. <https://doi.org/10.1016/j.conb.2012.11.015>.
- Sridharan, D., Levitin, D.J., Menon, V., 2008. A critical role for the right fronto-insular cortex in switching between central-executive and default-mode networks. *Proc. Natl. Acad. Sci. U.S.A.* 105, 12569–12574. <https://doi.org/10.1073/pnas.0800005105>.
- Stephan, K.M., Thaut, M.H., Wunderlich, G., Schicks, W., Tian, B., Tellmann, L., Homburg, V., 2002. Conscious and subconscious sensorimotor synchronization: prefrontal cortex and the influence of awareness. *Neuroimage* 15, 345–352. <https://doi.org/10.1006/nimg.2001.0929>.
- Stepp, N., Turvey, M.T., 2010. On strong anticipation. *Cognit. Syst. Res.* 11 (2), 148–164. <https://doi.org/10.1016/j.cogsys.2009.03.003>.
- Tanaka, H., Ishikawa, T., Lee, J., Kakei, S., 2020. The cerebro-cerebellum as a locus of forward model: a review. *Front. Syst. Neurosci.* 14 (19) <https://doi.org/10.3389/fnsys.2020.00019>.
- Taxali, A., Angstadt, M., Rutherford, S., Sripada, C., 2021. Boost in test–retest reliability in resting state fmri with predictive modeling. *Cerebr. Cortex* 31 (6), 2822–2833. <https://doi.org/10.1093/cercor/bhaa390>.
- Thaut, M.H., Demartin, M., Sanes, J.N., 2008. Brain networks for integrative rhythm formation. *PLoS One* 3, e2312. <https://doi.org/10.1371/journal.pone.0002312>.
- Todd, N.P., Lee, C.S., 2015a. The sensory-motor theory of rhythm and beat induction 20 years on: a new synthesis and future perspectives. *Front. Hum. Neurosci.* 9, 444. <https://doi.org/10.3389/fnhum.2015.00444>.
- Todd, N.P., Lee, C.S., 2015b. Source analysis of electrophysiological correlates of beat induction as sensory-guided action. *Front. Psychol.* 6, 1178. <https://doi.org/10.3389/fpsyg.2015.01178>.
- Tognoli, E., Kelso, J.A., 2014. The metastable brain. *Neuron* 81 (1), 35–48. <https://doi.org/10.1016/j.neuron.2013.12.022>.
- Toivainen, P., Burunat, I., Brattico, E., Vuust, P., Alluri, V., 2020. The chronnectome of musical beat. *Neuroimage* 216, 116191. <https://doi.org/10.1016/j.neuroimage.2019.116191>.
- Tops, M., Boksem, M.A., 2011. A potential role of the inferior frontal gyrus and anterior insula in cognitive control, brain rhythms, and event-related potentials. *Front. Psychol.* 2, 330. <https://doi.org/10.3389/fpsyg.2011.00330>.
- Tso, I.F., Rutherford, S., Fang, Y., Angstadt, M., Taylor, S.F., 2018. The “social brain” is highly sensitive to the mere presence of social information: an automated meta-analysis and an independent study. *PLoS One* 13 (5), e0196503. <https://doi.org/10.1371/journal.pone.0196503>.
- Tziortzi, A.C., Haber, S.N., Searle, G.E., Tsoumpas, C., Long, C.J., Shotbolt, P., Gunn, R. N., 2014. Connectivity-based functional analysis of dopamine release in the striatum using diffusion-weighted MRI and positron emission tomography. *Cerebr. Cortex* 24 (5), 1165–1177. <https://doi.org/10.1093/cercor/bhs397>.
- Uddin, L.Q., 2015. Salience processing and insular cortical function and dysfunction. *Nat. Rev. Neurosci.* 16 (1), 55–61. <https://doi.org/10.1038/nrn3857>.
- Uddin, L.Q., Nomi, J.S., Hebert-Seropian, B., Ghaziri, J., Boucher, O., 2017. Structure and function of the human insula. *J. Clin. Neurophysiol.* 34 (4).
- van den Heuvel, M.P., Sporns, O., 2013. Network hubs in the human brain. *Trends Cognit. Sci.* 17 (12), 683–696. <https://doi.org/10.1016/j.tics.2013.09.012>.
- van der Steen, M.C., Jacoby, N., Fairhurst, M.T., Keller, P.E., 2015a. Sensorimotor synchronization with tempo-changing auditory sequences: modeling temporal adaptation and anticipation. *Brain Res.* 1626, 66–87. <https://doi.org/10.1016/j.brainres.2015.01.053>.
- van der Steen, M.C., Keller, P.E., 2013. The ADaptation and Anticipation Model (ADAM) of sensorimotor synchronization. *Front. Hum. Neurosci.* 7, 253. <https://doi.org/10.3389/fnhum.2013.00253>.
- van der Steen, M.C., Schwartze, M., Kotz, S.A., Keller, P.E., 2015b. Modeling effects of cerebellar and basal ganglia lesions on adaptation and anticipation during sensorimotor synchronization. *Ann. N. Y. Acad. Sci.* 1337, 101–110. <https://doi.org/10.1111/nyas.12628>.
- Van Overwalle, F., 2009. Social cognition and the brain: a meta-analysis. *Hum. Brain Mapp.* 30 (3), 829–858. <https://doi.org/10.1002/hbm.20547>.
- Van Overwalle, F., Manto, M., Cattaneo, Z., Clausi, S., Ferrari, C., Gabrieli, J.D.E., Leggio, M., 2020. Consensus paper: cerebellum and social cognition. *Cerebellum* 19 (6), 833–868. <https://doi.org/10.1007/s12311-020-01155-1>.
- Vorberg, D., Schulze, H.-H., 2002. A two-level timing model for synchronization. *J. Math. Psychol.* 46, 56–87.
- Vorberg, D., Wing, A.M., 1996. Modeling variability and dependence in timing. In: Keele, S.W. (Ed.), *Handbook of Perception and Action*, vol. 2. Academic Press, London, pp. 181–262.
- Vuust, P., Heggli, O.A., Friston, K.J., Kringelbach, M.L., 2022. Music in the brain. *Nat. Rev. Neurosci.* <https://doi.org/10.1038/s41583-022-00578-5>.
- Vuust, P., Roepstorff, A., Wallentin, M., Mouridsen, K., Ostergaard, L., 2006. It don't mean a thing... Keeping the rhythm during polyrhythmic tension, activates language areas (BA47). *Neuroimage* 31 (2), 832–841. <https://doi.org/10.1016/j.neuroimage.2005.12.037>.
- Wang, R., Liu, M., Cheng, X., Wu, Y., Hildebrandt, A., Zhou, C., 2021. Segregation, integration, and balance of large-scale resting brain networks configure different cognitive abilities. *Proc. Natl. Acad. Sci. USA* 118 (23), e2022288118. <https://doi.org/10.1073/pnas.2022288118>.
- Witt, S.T., Laird, A.R., Meyerand, M.E., 2008. Functional neuroimaging correlates of finger-tapping task variations: an ALE meta-analysis. *Neuroimage* 42, 343–356. <https://doi.org/10.1016/j.neuroimage.2008.04.025>.
- Wolpert, D.M., Doya, K., Kawato, M., 2003. A unifying computational framework for motor control and social interaction. *Philos. Trans. R. Soc. Lond. Ser. B Biol. Sci.* 358, 593–602. <https://doi.org/10.1098/rstb.2002.1238>.
- Wolpert, D.M., Kawato, M., 1998. Multiple paired forward and inverse models for motor control. *Neural Network* 11, 1317–1329.